Cerebral Cortex February 2009;19:331-348
doi:10.1093/cercor/bhn085
Advance Access publication May 30, 2008

Intrinsic Signal Imaging of Deprivation-Induced Contraction of Whisker Representations in Rat Somatosensory Cortex

Patrick J. Drew[1] and Daniel E. Feldman[2]

Section of Neurobiology, Division of Biological Science, University of California, San Diego, La Jolla, CA 92093-0357, USA
[1]Present address: Department of Physics, University of California, San Diego, La Jolla, CA 92093-0374, USA.
[2]Present address: Department of Molecular & Cell Biology, University of California-Berkeley, Berkeley, CA 94720, USA.

In classical sensory cortical map plasticity, the representation of deprived or underused inputs contracts within cortical sensory maps, whereas spared inputs expand. Expansion of spared inputs occurs preferentially into nearby cortical columns representing temporally correlated spared inputs, suggesting that expansion involves correlation-based learning rules at cross-columnar synapses. It is unknown whether deprived representations contract in a similar anisotropic manner, which would implicate similar learning rules and sites of plasticity. We briefly deprived D-row whiskers in 20-day-old rats, so that each deprived whisker had deprived (D-row) and spared (C- and E-row) neighbors. Intrinsic signal optical imaging revealed that D-row deprivation weakened and contracted the functional representation of deprived D-row whiskers in L2/3 of somatosensory (S1) cortex. Spared whisker representations did not strengthen or expand, indicating that D-row deprivation selectively engages the depression component of map plasticity. Contraction of deprived whisker representations was spatially uniform, with equal withdrawal from spared and deprived neighbors. Single-unit electrophysiological recordings confirmed these results, and showed substantial weakening of responses to deprived whiskers in layer 2/3 of S1, and modest weakening in L4. The observed isotropic contraction of deprived whisker representations during D-row deprivation is consistent with plasticity at intracolumnar, rather than cross-columnar, synapses.

Keywords: barrel, imaging, intrinsic signal, map plasticity, optical, whisker

Introduction

Sensory experience drives plasticity in cortical sensory maps. In classical map plasticity, deprivation of a subset of inputs causes representations of deprived inputs to contract within maps, and spared inputs to expand (Buonomano and Merzenich 1998; Fox 2002; Feldman and Brecht 2005). One strategy for inferring the specific sites and learning rules for cortical map plasticity is to examine the spatial profile of expansion and contraction of inputs within maps. For example, spared active inputs expand preferentially into neighboring cortical columns representing other spared, temporally correlated inputs, rather than into columns representing noncorrelated or deprived inputs (Diamond et al. 1993, 1994; Armstrong-James et al. 1994; Wang et al. 1995; Lebedev et al. 2000). Indeed, spared inputs may actually withdraw from these deprived columns (Wallace and Sakmann 2007). These anisometric effects suggest that expansion of active inputs involves correlation-based (Hebbian) learning rules, perhaps on intracortical, cross-columnar synaptic connections (Wang et al. 1995; Buonomano and Merzenich 1998; Gilbert 1998; Lebedev et al. 2000; Song and Abbott 2001; Fox 2002; Wallace and Sakmann 2007). In contrast, whether contraction of deprived inputs within maps is similarly anisometric, and therefore likely to involve similar learning rules and sites of plasticity, is unknown.

Here we investigate this issue by measuring how representations of deprived whisker inputs contract during whisker map plasticity in rat primary somatosensory (S1) cortex. Rats have ~30 large whiskers on each side of the face, represented in an isomorphic functional map within S1 (Petersen 2003). Trimming or plucking a subset of whiskers for several weeks causes the representation of deprived whiskers to weaken and contract within the map, as measured by extracellular recording of whisker-evoked spikes or metabolic imaging (Simons and Land 1987; Fox 1992; Glazewski and Fox 1996; Kossut 1989; Wallace and Fox 1999; Skibinska et al. 2000; Feldman and Brecht 2005).

To examine how deprived representations contract, we selectively deprived the D-row of whiskers by plucking or trimming for 6–10 days in juvenile rats. This duration of deprivation weakens deprived inputs but does not drive strengthening of spared inputs, which is a slower process (Fox et al. 1996). In this paradigm, each deprived column is surrounded by 2 spared columns (adjacent, intact C- and E-row whiskers) and 2 deprived columns (adjacent deprived whiskers within the D-row). Row-based deprivation paradigms have been used to identify cellular mechanisms of plasticity at S1 synapses (Finnerty et al. 1999; Allen et al. 2003; Shepherd et al. 2003; Bender et al. 2006; Cheetham et al. 2007), but the effect on representation of deprived whiskers is not known. After a short period of whisker regrowth to allow whisker-evoked responses to be measured, we assayed the functional representation of each whisker using intrinsic signal optical imaging, a hemodynamic measure of neural activity that has been used to visualize whisker maps (Grinvald et al. 1986; Masino et al. 1993; Peterson et al. 1998; Polley et al. 1999, 2004; Masino 2003; Dubroff et al. 2005), and map plasticity (Polley et al. 1999). The intrinsic signal correlates with sensory-evoked spiking on the ~100 μm spatial scale (Ts'o et al. 1990), and reports the region of S1 (primarily, layer 2/3) that is functionally activated by each whisker.

D-row deprivation was found to cause weakening and contraction of deprived whisker inputs in S1. Contraction was spatially uniform, with no sign of preferential withdrawal from spared versus deprived neighboring columns. Single-unit extracellular recordings confirmed these findings, and showed that plasticity took place primarily in L2/3, not L4. These results are not readily consistent with correlation-based plasticity of horizontal, cross-columnar projections, and instead are consistent with the hypothesis that weakening reflects a primary locus of plasticity on intracolumnar synapses within

the deprived column, as indicated by recent cellular findings (Allen et al. 2003; Shepherd et al. 2003; Bender et al. 2006; Cheetham et al. 2007).

Methods

Experiments were done in accordance with National Institutes of Health policies and approved by the UCSD Institutional Animal Care and Use Committee. Thirty-nine Long–Evans rats (age 32–46 days, 110–210 g, both sexes) were used.

Whisker Deprivation Protocol

Animals were housed in litters until 20 days of age, when the D-row of whiskers (D1–D5 and gamma) on the right side of the face were either plucked gently with forceps (14 rats) or trimmed to the level of the fur (9 rats). Plucking and trimming were performed under transient general isoflurane anesthesia (Allen et al. 2003; Bender et al. 2006). Care was taken during plucking not to damage the follicle. Whiskers were replucked or retrimmed every other day until P26 (for plucked animals) or P30 (for trimmed animals), when whiskers were allowed to regrow for 5–16 days before recording, in order to allow whisker-evoked responses to be measured. Whiskers typically regrew 1–2 mm per day before P30, and more slowly after P30. Deprivation ended earlier for plucked rats than trimmed rats because plucked whiskers often took longer to regrow. Mean whisker length on the day of recording was: plucked D1, 10.6 ± 1.2 mm (SE); trimmed D1, 4.0 ± 0.4 mm; plucked D2, 9.9 ± 0.9 mm; trimmed D2, 8.9 ± 1.3 mm. Regrown whiskers were still much shorter than control, nondeprived whiskers (~30 mm), suggesting that regrowth may be considered a period of continuing, albeit diminished, deprivation. Animals were weaned at P20 and housed in standard laboratory cages with one to 2 littermates. Control rats were nondeprived age-matched animals (n = 13) or sham-deprived littermates cohoused with deprived animals (n = 3). Where data from plucked and trimmed rats are pooled together, we refer to plucked/trimmed whiskers as "deprived" whiskers. Rats with trimmed or plucked whiskers explore, interact, whisk, and gain weight normally (Diamond et al. 1993; D.E.F., unpublished data), and thus whisker deprivation is an effective, innocuous method of altering sensory experience.

Surgery

Rats were anesthetized with urethane (1.5 g/kg, 20% in sterile saline, injected intraperitoneally [i.p.]), and body temperature was maintained with a feedback-controlled heating blanket. A small post was attached to the skull with dental cement to secure the head without pressure points. A circular imaging chamber (5 mm internal diameter, 1.5–2 mm height) was cemented tangential to the skull 2.5 mm caudal and 5.5 mm lateral from bregma. The skull was thinned to approximately 100 μm within the chamber. The chamber was filled with silicon oil (DC200, Sigma, St. Louis, MO) to render the skull transparent, and imaging was performed through the oil. Care was taken to keep the anesthesia level constant during the course of the experiment, as measured by breathing rate and absence of limb withdrawal reflexes. Anesthesia was maintained with supplemental doses of urethane (15% of original dose, i.p.) whenever limb withdrawal responses appeared, whisker movements were observed, or breathing rate exceeded 120 breaths/min. Recording sessions were terminated if there was a noticeable change in breathing rate or pattern or anesthetic level. Because preliminary experiments indicated that lactated Ringer's interfered with measurement of the intrinsic signal, lactated ringers (Baxter, Deerfield IL; 1–2 ml, i.p.) was administered to ensure adequate hydration at the conclusion of the imaging portion of each experiment (~3 h after initial surgery), before extracellular recordings began.

Whisker Stimulation for Intrinsic Signal Imaging

Whisker stimulation was performed using a 3 × 3 array of 9 independent, computer-controlled piezoelectric bimorph elements (T215-H4CL-103X, 1.25" × 0.125" × 0.015"; Piezo Systems, Inc., Cambridge, MA), coupled to lightweight plastic tubes into which individual whiskers were fixed using rubber cement (Drew and Feldman 2007). Whisker deflection was controlled by custom routines in Igor (Wavemetrics, Lake Oswego, OR). Individual whiskers were deflected with 2.2° amplitude ramp–hold–return deflections (caudal initial deflection, 115 μm amplitude, applied 3 mm from the face, 4 ms ramp, 60 ms hold, 4 ms return ramp, ramp/return velocity 28.75 mm/s [550°/s]). Piezo movement was calibrated optically to minimize ringing (ringing was <5% of total displacement amplitude) and to verify independence of movement between piezos (>20 dB attenuation between neighboring piezos). For intrinsic imaging, individual whiskers were deflected with a train of 8 ramp–hold–return deflections, presented at 8 Hz (the "train stimulus"). This frequency of whisker stimulation has been shown to produce the most localized activation of the intrinsic signal (Sheth et al. 1998) and is near the frequency of natural whisking (Welker 1964). Arc 1 (C1–D1–E1) was imaged first by applying the train stimulus to each of the 3 whiskers in the arc, in an interleaved pattern (e.g., C1 then D1 then E1), with 20 s between stimuli. Forty-five to 60 (usually 50) repetitions were performed. Arc 2 (C2–D2–E2) was imaged separately using the same procedure.

Acquisition of Intrinsic Images

Images were acquired with a 12-bit 1M60 camera (Dalsa, Waterloo, ON) with a macroscope composed of 2 50-mm camera lenses (Ratzlaff and Grinvald 1991). An initial image was taken of the cortical vasculature to enable alignment of intrinsic signal images with cytochrome oxidase (CO) barrel maps and electrophysiological recording sites (see below). The camera was then focused down 400–600 μm below the surface. Images (256 pixels × 256 pixels, 3.2 mm × 3.2 mm) were acquired at 30–50 fps using custom-written LabView software (National Instruments, TX) and binned into 0.5-s bins for online analysis. The frame rate was adjusted in each experiment to maximize the amount of illumination without saturating the camera. For intrinsic signal images, the skull was illuminated with red (630 nm) light emitting diodes powered by a stable light source (Intralux dc-1100, Volpi, Switzerland). For imaging the surface vasculature, green (525 nm) light was used.

Analysis of Intrinsic Images

Imaging data were analyzed off-line using custom routines in Matlab (Mathworks, Natick, MA). Individual image frames acquired at 30–50 fps were binned into 0.5-s frames. The stimulus started at the beginning of the 0-s frame and ended at the beginning of the 1-s frame (Fig. 1). To quantify whisker responses, the 2 frames spanning 0.5–1.5 s after stimulus onset were averaged, and divided by the average of 2 baseline frames (Chen-Bee et al. 2000). The resulting image was spatially filtered with a 2-dimensional Gaussian (37.5 μm standard deviation). The median of the entire image was subtracted to minimize the effects of slow, global fluctuations in luminance (Mayhew et al. 1996), including rundown (Gurden et al. 2006). Note that median subtraction will tend to oppose the observed shrinkage in whisker response areas (WRAs) of deprived whiskers. The WRA for the stimulated whisker in each frame was quantified as the area with pixel values below absolute thresholds of −1.5, −2.0, −2.5, −3.0, and -3.5×10^{-4} (fractional decrease in reflectance) (Polley et al. 2004). In some cases, dark blood vessels that clearly extended outward from the WRA were masked out prior to WRA calculation. When masking was performed, the masked area was typically <0.2 mm^2. In a few cases, blood vessel artifacts were too numerous for accurate estimation of the WRA, and the WRA was excluded from the data set. Across animals, there was no relationship between breathing rate and the size of the WRA (slope of the linear regression between WRA area for control D1 whisker and breathing rate, $m = -0.005 mm^2/(breath/min)$, $r^2 = 0.02$, not significantly different from 0, $P > 0.05$). Because breathing rate correlates with anesthetic depth (Erchova et al. 2002), this suggests that the slight variations in anesthetic depth that occur with this urethane anesthesia regime do not strongly impact WRA area. There was also no effect of animal weight on WRA area (slope of regression between WRA area for control D1 whisker and weight, $m = 0.008 mm^2/g$, $r^2 = 0.24$, not significantly different from 0, $P > 0.05$).

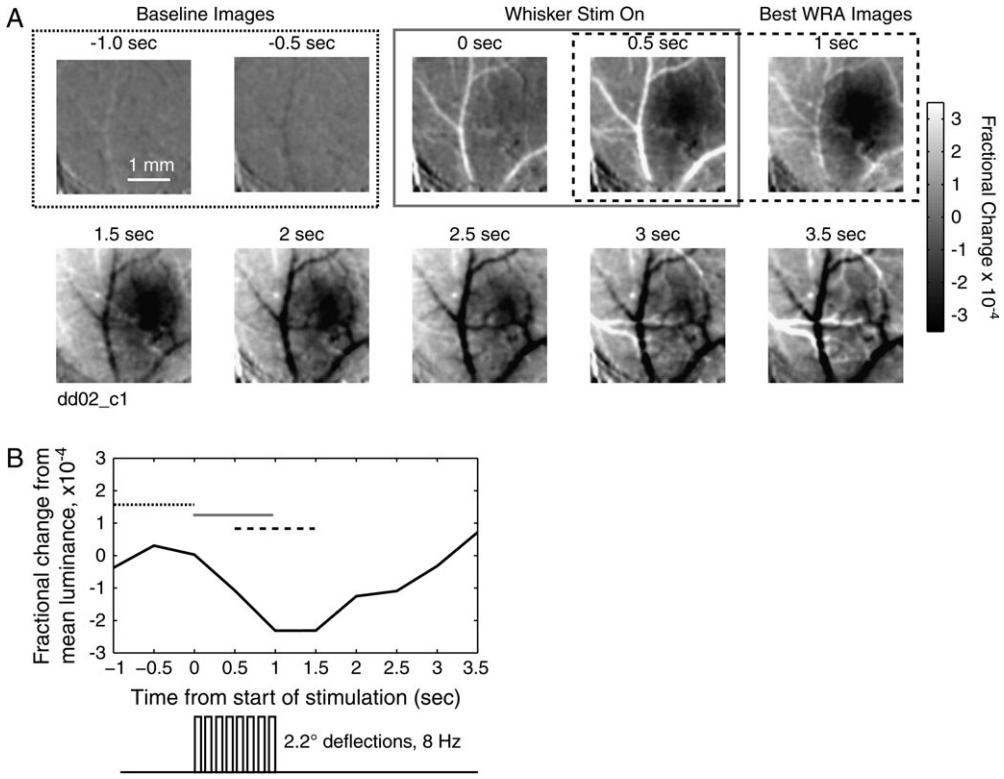

Figure 1. Whisker-evoked intrinsic signal in S1. (*A*) Stimulation consists of one second of baseline (outlined in dotted line), followed by one second of 8-Hz stimulation of the C1 whisker (gray line). Each image is an average over 0.5 s, and divided by the average image obtained during the baseline period (−1 to 0 s). The fractional change is indicated in gray scale, with black denoting a decrease in reflectance, white an increase. The images of the barrel least disrupted by blood vessels are found between 0.5 and 1.5 s after the start of stimulation (in dashed line box). Caudal is to the right, medial up. (*B*) Average reflectance over the entire image. Mean reflectance of during the baseline second is subtracted out. Dotted bar denotes baseline frames, gray time of whisker stimulation and dashed line the time over which the images are averaged for analysis. Note the dip in reflectance following stimulation and the subsequent rebound.

The geometrical center of each individual WRA was defined as the unweighted mean location of all the points within the -1.5×10^{-4} contour. The peak of the WRA was defined as the largest decrease in fractional reflectance of any single pixel within the WRA. The eccentricity of individual WRAs was calculated as the ratio of the smallest to the largest principle components of the area enclosed by the -1.5×10^{-4} threshold, with all points within the contour being weighted equally. This eccentricity measure varies between 1 (a circular WRA) and 0 (a line). For generating the ellipsoid representation of the WRAs (Fig. 6), the principal components of the average population WRAs at the -1.5×10^{-4} contour were used to obtain the orientation and eccentricity of an ellipsoid whose area was that of the mean area of the -1.5×10^{-4} contour. The -1.5×10^{-4} threshold contour was used for these measures because it allowed measurements to be made in weak WRAs of deprived whiskers, which often did not reach higher absolute thresholds.

For several analyses, we calculated the shape or position of WRAs relative to the arc and row axes of the anatomical barrel map, as determined from CO staining in each animal. To calculate the relative extent of each WRA along the anatomical whisker row axis versus the whisker arc axis, we calculated the mean intensity of the WRA along the anatomically determined D-row axis (the "row axis projection"), and the mean intensity along the perpendicular axis (the "arc axis projection"), and fit these projections with Gaussians. The relative extent of the WRA along row versus arc axes was defined as the ratio of the standard deviation of these Gaussians. WRAs with area <0.2 mm^2 were excluded because they often had nonunimodal axis projections which could not be fit with Gaussians. As a second measure of relative extent of WRAs along the row axis of the anatomical barrel map, we calculated the inner product of the largest principal component of the WRA and the D-row axis, and divided this by the square root of the area enclosed in the -1.5×10^{-4} contour. Changes in this ratio with deprivation indicate nonisometric shrinkage of WRAs; lack of change of this ratio indicates isometric shrinkage.

To generate the average WRA images in Figure 5*B*, individual WRAs were spatially aligned on the centroids of their -1.5×10^{-4} contour, and rotated so that the anatomical D-row axes determined from CO barrel maps (see below) were aligned. The average pixel intensity was then calculated across the aligned WRAs. This calculation was done separately for each control, plucked, and trimmed whisker. Pixel intensity for each average WRA was then normalized to the peak pixel of the average WRA for the corresponding control whisker. Each WRA was plotted using a separate color channel (red, green, or blue). The average WRAs were plotted centered on their average Cartesian coordinates relative to each other. Areas of overlap appear as color mixtures, with luminance representing the amount of activation. WRA images from 6 rats in which CO barrel maps were not obtained were excluded from this analysis.

Because much of the data were nonnormally distributed, the Mann–Whitney *U* test was used for tests of statistical significance, unless otherwise indicated. Reported numbers are mean ± standard error.

Extracellular Single-Unit Recording

In a subset of animals, extracellular recordings of single-unit activity were made from specific cortical sites after intrinsic signal imaging. The silicone oil, thinned skull and dura were removed, taking great care not to damage the cortex. The imaging chamber was filled with 4-(2-hydroxyethyl)-1-piperanzineethanesulfonic acid (HEPES)-buffered Ringer's solution (Jacob et al. 2007). Tungsten electrodes (2–4 MΩ, FHC, Bowdenham, ME) were inserted radially into the cortex. Signals were preamplified (1000× gain, DAM-50, WPI, Sarasota, FL), band pass filtered (0.5–10 kHz, Krohn-Hite 3364, Brockton, MA), further amplified (3×, Brownlee 410, San Jose, CA), and digitized at 32 kHz using a 12-bit acquisition board (National Instruments) running custom-written routines in Igor (Wavemetrics, Lake Oswego, OR).

Recording penetrations were made in the C1, D1, E1, D2, and C2 barrel columns. Recording sites were selected based on the appearance of well-isolated units as determined by online visual inspection of voltage waveforms, using a random sequence of individual whisker deflections (9 whiskers centered around the expected principal whisker) as search stimulus. Recording sites were separated by >50 μm. Single units were isolated off-line using the method of Fee et al. (1996), implemented in Matlab by S. Mehta and S. Jadhav. This method uses a clustering algorithm to separate units based on the entire spike waveform (1.5 ms) (Celikel et al. 2004; Gabernet et al. 2005). Isolated units were required to have < 1% of spikes with an interspike interval (ISI) < 1 ms and at least 200 total spikes within the recorded sweeps, which corresponds to mean firing rate >0.22 Hz. Only putative regular spiking units, having a combined action potential and afterhyperpolarization duration of longer than 0.75 ms (Swadlow 1989; Gabernet et al. 2005) were included in the analysis.

At each recording site, neural responses were measured to 50 repetitions of randomly interleaved deflection of 9 adjacent whiskers (for recordings in E1, D1, or C1 columns, the 9 whiskers were beta, C1, C2, gamma, D1, D2, delta, E1, and E2; for recordings in E2, D2, or C2 columns, the whiskers were E1, E2, E3, D1, D2, D3, C1, C2, and C3). Whisker stimuli were single ramp–hold–return deflections (4 ms rise time, 100 ms hold, 4-ms fall time, otherwise identical to the whisker deflections used for intrinsic signal imaging), for comparison with prior studies (e.g., Simons 1978; Simons and Land 1987). A 2-s interstimulus interval was used to prevent response adaptation.

On-responses were defined as spikes occurring 5–25 ms after whisker deflection onset. Off-responses were defined as responses occurring 105–125 ms after deflection onset, with background firing (measured 0–200 ms before whisker deflection) subtracted. OFF/ON response ratios (Simons and Land 1987) were calculated by dividing the off response by the on response without background rates subtraction to prevent negative values. Response latency was calculated as Foeller et al. (2005). All peristimulus time histograms (PSTHs) use 1-ms bins.

Histology

To align intrinsic signal images with barrel maps when single-unit recordings were not performed, 3–4 fiduciary marks were made after imaging, using an inked pin (0.05 mm diameter, ~0.5 mm spacing) inserted radially 1–2 mm into the cortex. The resulting ink spots on the brain surface were photographed and aligned with the intrinsic signal map. The animal was euthanized, the brain was removed and fixed in 4% paraformaldehyde in phosphate buffer (0.1 M, pH 7.4) and sunk in 30% sucrose in 4% paraformaldehyde. The cortex was flattened, sectioned at 100 μm on a freezing microtome, and stained for CO (Fox 1992). CO-stained barrels were traced from these sections, and the fiduciary marks (pinholes) were identified in these sections and used to align the CO-stained barrel map with the intrinsic signal map.

To reconstruct the location of electrophysiological recording penetrations, and to align intrinsic signal images with barrel maps in experiments in which single-unit recordings had been made, small electrolytic lesions (3 μA, 10 s each) were made via the tungsten recording electrode in layer 4 (depth: 700–850 μm below the pial surface) at 2–4 defined locations relative to the surface vasculature and microdrive coordinates. During tissue processing, care was taken to preserve surface vasculature in the most superficial section through flattened cortex. Barrels and marking lesions in L4 were traced from CO-stained sections. Intrinsic signal maps were aligned with the barrel maps using lesions, and by comparing in vivo images of surface vasculature with the vascular pattern preserved in the superficial histological section.

Results

Intrinsic Imaging of Whisker Responses in S1 Cortex

Intrinsic signal optical imaging (Grinvald et al. 1986) was used to assess the topography of the functional whisker map in S1 cortex of urethane anesthetized, 32- to 46-day-old rats. After thinning the skull over S1 cortex, red light reflectance images were acquired and binned into 0.5-s frames before, during, and after a 1-s long train of whisker deflection. Dividing all frames by the mean baseline frame (calculated over the 1 s prior to whisker deflection) revealed localized changes in cortical reflectance following whisker stimulation (see Methods for details). An example, averaged over 50 whisker deflection trains, is shown in Figure 1. The strongest decrease in reflectance, with the least contamination by signals from blood vessels, was observed in the 2 frames beginning 0.5 and 1.0 s after stimulation onset (Fig. 1*A*). Images gathered during this time period were used for all subsequent analysis. This signal (the "initial dip") recovered and reversed after approximately 3 s (Fig. 1*B*). The magnitude and dynamics of the intrinsic signal were consistent with prior studies in S1 (see Chen-Bee et al. 2000).

In each rat, we measured the cortical area activated by a whisker, which we term the "whisker response area" (WRA), for each of the C1, D1, E1, C2, D2, and E2 whiskers. WRAs for whiskers within arc 1 (C1, D1, and E1) were measured simultaneously by interleaved deflection of these whiskers 45–60 times, followed by similar imaging of arc 2. The WRA for each whisker was defined from Gaussian-smoothed images (see Methods) as the image area in which reflectance was decreased by at least a factor of -1.5×10^{-4} relative to baseline (dark gray to black in Fig. 1*A*). For rats with normal whisker experience, WRAs for these 6 whiskers had a mean size of 1.00 ± 0.06 mm^2 and a peak magnitude (the fractional change in reflectance measured at the most active pixel) of $-4.0 \pm 0.12 \times 10^{-4}$. WRA area did not significantly vary across the range of ages studied (P32–46), except for D2, which increased by ~50%. The internal shape of the WRA was determined by applying progressively higher reflectance thresholds, which enclose progressively less area. Examples of WRAs for C1, D1, and E1 whiskers in 3 representative control rats are shown in Figure 2 (top), relative to the anatomical barrel map measured from CO-stained sections from these same animals (see Methods for CO staining and alignment; and see Supplementary Fig. 1 for raw intrinsic signal images). The WRA for each whisker was typically much larger than the anatomical cortical column corresponding to that whisker. This has been proposed to reflect the fact that each whisker evokes "principal whisker" spiking responses in its corresponding column, as well as "surround whisker" spiking responses in neighboring columns, both of which generate intrinsic signal (Peterson et al. 1998; Masino 2003). Intrinsic signal may also reflect whisker-evoked glutamate release (Gurden et al. 2006), which occurs over a large, multicolumn area (Moore and Nelson 1998; Brecht et al. 2003). However, the most active region within each WRA tended to align near the center of the whisker's anatomical barrel column (the accuracy of this alignment is analyzed below). WRAs were typically elliptical, spreading further within the barrel row than across rows (Fig. 2*B*, *E*, *F*). This is consistent with voltage-sensitive dye imaging of whisker representations (Petersen et al. 2003; Wallace and Sakmann 2007) and may be due to preferential spread of cross-columnar axons along the row axis (Bernardo et al. 1990; Kim and Ebner 1999; Petersen et al. 2003).

Effect of D-Row Whisker Deprivation on Intrinsic Signal Maps

To test how whisker deprivation altered the functional whisker map in S1, we plucked or trimmed the D-row of whiskers

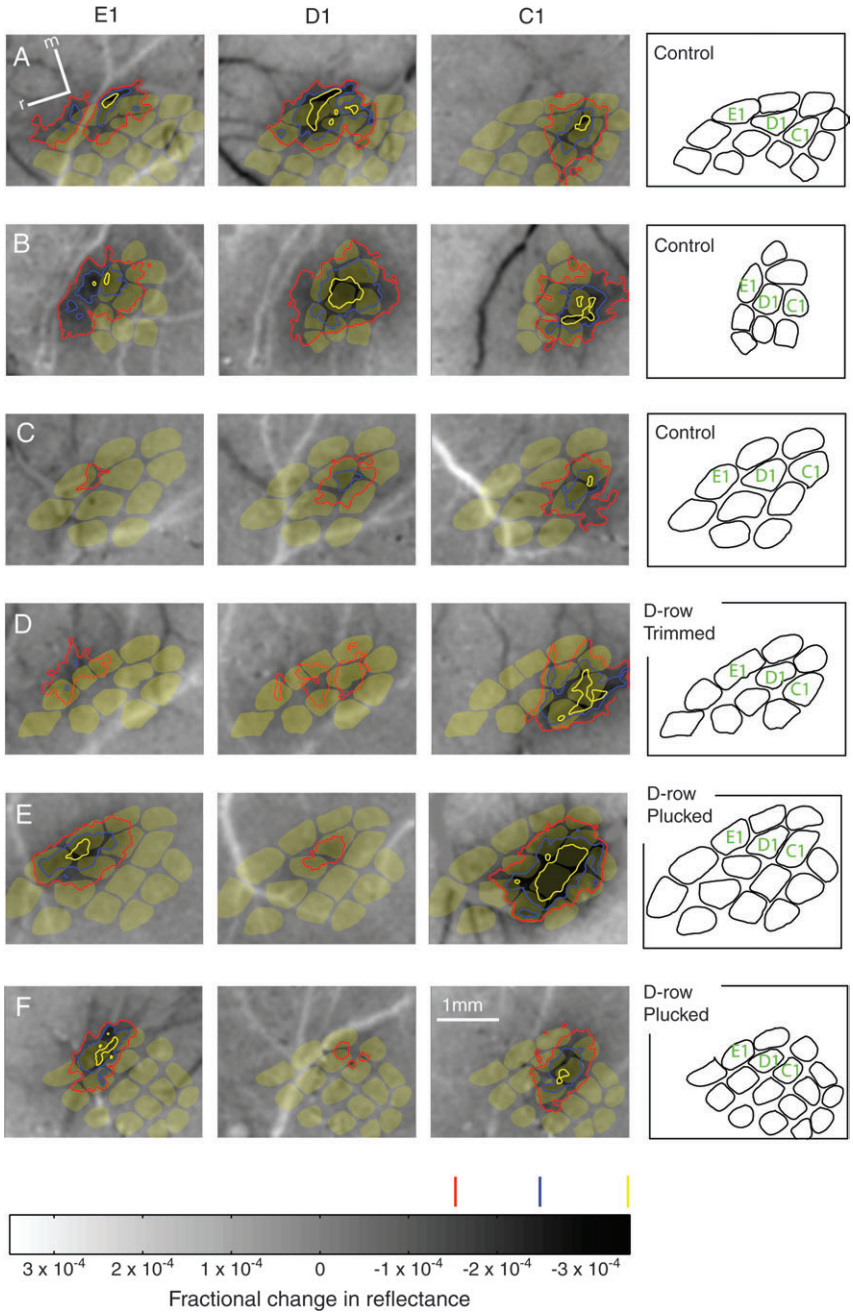

Figure 2. Example WRAs in control and D-row plucked rats. Each panel shows a gray scale image of whisker-evoked changes in luminance, relative to baseline (darker values denote decreased reflectance and increased neural activity). Dark and light streaks are blood vessels. WRAs are indicated by the different colored contours, which enclose areas of progressively stronger intrinsic signal, as shown on gray scale bar at bottom. Red indicates the lowest threshold for whisker-evoked intrinsic signal (pixel values -1.5×10^{-4}), and yellow the highest threshold (-3.5×10^{-4}). Contours with intermediate thresholds were calculated for analysis (e.g., Fig. 3), but are not shown here. WRAs are overlaid on anatomical barrel maps measured from CO-stained histological sections in the same animal (shown in yellow). See SupplementaryFigure 1 for unobstructed versions of the intrinsic signal images. (*A–C*) Three representative control animals. m, medial. r, rostral. (*D*) Representative rat that had the D-row of whiskers trimmed. (*E*, *F*) Two representative rats that had the D-row plucked.

(D1–D5 and gamma) on the right side of the face beginning at P20, and continuing every other day until P26 (for plucking, $n = 12$ rats) or P30 (for trimming, $n = 9$ rats). Whiskers were then allowed to partially regrow (6–15 days), in order to allow cortical responses to deprived whiskers to be measured. This and similar row-based deprivation protocols are known to drive synaptic plasticity at specific S1 synapses (Bender et al. 2006; Finnerty et al. 1999; Allen et al. 2003; Shepherd et al. 2003), but their effects on deprived whisker representations have not been measured. Based on standard Hebbian plasticity mechanisms and prior results from other whisker deprivation protocols, the cortical response to the deprived whiskers would be expected to decrease (Glazewski et al. 1996; Wallace and Fox 1999; Feldman and Brecht 2005).

We used intrinsic signal imaging to measure WRAs for single deprived and spared whiskers in deprived rats, and compared them to WRAs for corresponding whiskers in age-matched control rats with normal whisker experience. We found that

the representation of deprived D-row whiskers was reduced relative to control rats. Figure 2*B* (bottom) shows examples of WRAs for C1, D1, and E1 whiskers from 3 representative rats in which the D-row of whiskers was plucked or trimmed. Though the mean area of WRAs across all whiskers varied from rat to rat, D1 whisker WRAs were substantially smaller and weaker in D-row deprived rats relative to control rats, whereas WRAs for the spared C1 and E1 whiskers were relatively normal in size and strength. (See SupplementaryFig. 1 for raw intrinsic signal images.)

The effect of D-row deprivation on size of WRAs is quantified in Figure 3. For each WRA in each rat, we calculated the pixel area enclosed by each of 5 absolute contour thresholds (–1.5, –2, –2.5, –3, and –3.5 × 10^{-4} change in reflectance). We then averaged across rats to determine the average area enclosed by each threshold, for each whisker (E1–2, D1–2, and C1–2) (Chen-Bee et al. 2000; Polley et al. 2004). Results showed a marked reduction in WRA size for the deprived whiskers (D1 and D2), at all thresholds, relative to control rats. At the lowest absolute threshold (–1.5 × 10^{-4}) the area of the D1 WRA was significantly reduced by trimming or plucking, relative to control rats (control: 0.97 ± 0.13 mm^2, plucked: 0.25 ± 0.06, $P <$ 0.0002 versus control; trimmed: 0.56 ± 0.14, $P < 0.02$ versus control, Mann–Whitney U test). Similarly, the area of the D2 WRA was reduced significantly by plucking (control: 1.18 ± 0.12 mm^2, plucked: 0.58 ± 0.14 mm^2, $P < 0.008$), and trimming caused a strong nonsignificant trend for reduction (trimmed: 0.62 ± 0.24, $P < 0.07$ vs. control). Spared C- and E-row whiskers in D-row deprived rats were not changed in WRA area, relative to control ($P > 0.05$ in all cases). Thus, D-row deprivation shrank the functional representations of deprived D-row whiskers, but did not change the representation of spared C- and E-row whiskers.

Shrinkage of D-row whisker WRAs was also evident in the spatial width of WRAs determined from Gaussian fits. D-row plucking reduced the Gaussian width of D1 and D2 WRAs measured along arc and row axes (control: D1 arc 444 ± 36 μm, D1 row 536 ± 49 μm, D2 arc 491 ± 40 μm, D2 row 639 ± 40 μm; plucked: D1 arc 197 ± 56 μm, $P < 0.001$, D1 row 265 ± 80 μm, $P <$ 0.04, D2 arc 351 ± 64 μm, $P < 0.17$, D2 row 462 ± 84 μm, $P <$ 0.04). D-row trimming also significantly reduced D1 WRA width, and caused a nonsignificant trend for reduction in D2 WRA width (data not shown). There was no correlation between D1 WRA area and total duration of plucking or trimming, including the partial regrowth period (range: 12–20 days for plucking, 14–25 days for trimming; regression slope: 0.06 mm^2/day, $r^2 = 0.01$, $P > 0.05$, $n = 19$ animals). The magnitude of D2 WRA contraction during plucking or trimming was similarly independent of duration of deprivation (data not shown). Thus, the magnitude of plasticity, as measured by WRA area, appeared stationary over the range of deprivation durations that were tested.

How much deprived D-row whisker representations shrank can be visualized by calculating the mean WRA, across all animals, for each measured whisker within arc 1 or arc 2 (Fig. 3*B*). To do this, individual WRAs were aligned at their respective centroids, rotated so that the anatomically determined D-row axes were aligned, and then averaged. Maximal intensities of each WRA were normalized by the peak of the corresponding average control WRA. Each whisker was given a color (E green, D red, and C blue) and the 3 WRAs in an arc were overlaid. Yellow and purple regions are formed when E and D and D and C overlap, respectively. This analysis indicates that deprivation greatly reduced the extent and intensities of WRAs of deprived whiskers, but did not alter the extents of spared whiskers appreciably.

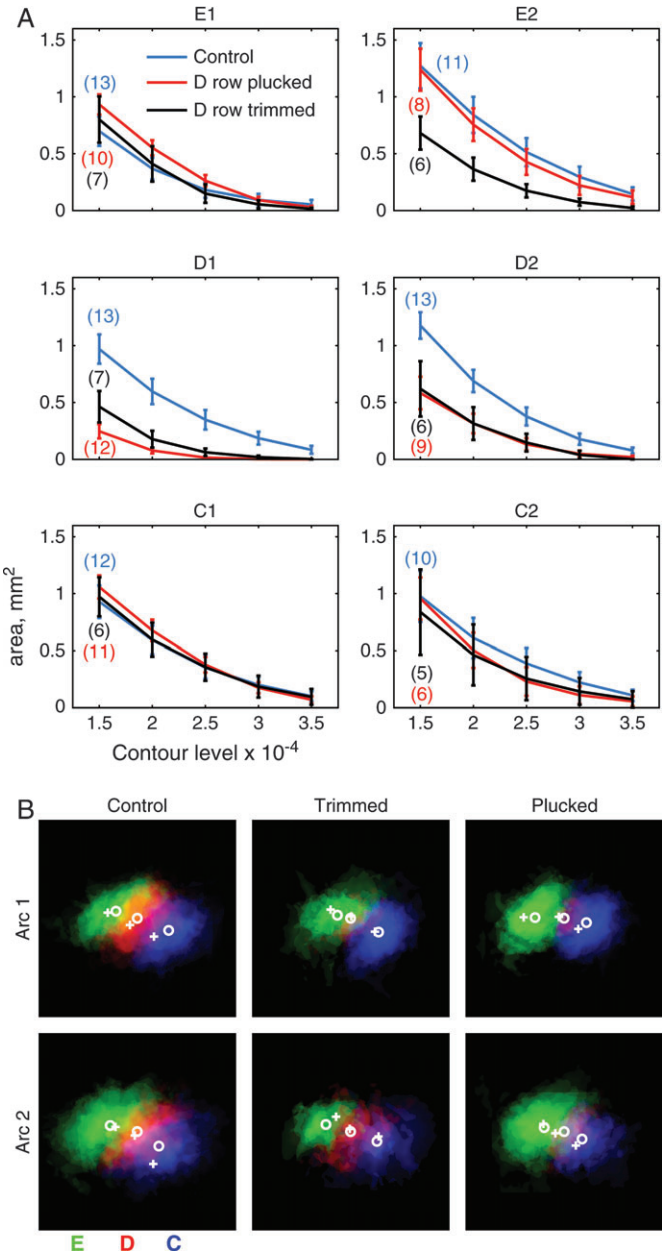

Figure 3. Quantitative effects of whisker deprivation on WRAs. (*A*) Mean WRA area as a function of contour threshold. Blue, control rats; Red, D-row plucked, black, D-row trimmed. Bars show standard error. (*B*) Overlay of averaged WRAs for C1, D1, and E1 whiskers (top row) and C2, D2, and E2 whiskers (bottom row), from control (left), D-trimmed (center) and D-plucked (right) animals. WRAs from each animal were aligned at their centers and rotated to align the anatomically determined D-row axis before averaging. The average spacing of the anatomical barrel centers was used to arrange the WRAs. E row is green, D is red, and C is blue. Color mixtures indicate areas of overlap. Deprivation reduced average D-row WRAs in size and intensity. White circles indicate average centers of WRAs, white crosses indicate averaged centers of barrel columns.

Deprivation also decreased the peak strength of the intrinsic signal in the most active region of the WRA. Peak strength of a WRA was defined as the largest decrease in reflectance,

relative to baseline, at any pixel within the WRA (Chen-Bee et al. 2000; Polley 2004). D-row plucking and trimming substantially decreased peak WRA strength relative to controls, for both D1 and D2 whiskers (Fig. 4) (D1 peak strength: control $-3.9 \pm 0.27 \times 10^{-4}$, plucked $-2.3 \pm 0.33 \times 10^{-4}$; $P < 0.001$ vs. control, *t*-test; trimmed $-2.5 \pm 0.48 \times 10^{-4}$, $P < 0.01$ vs. control; D2 peak strength: control $-4.2 \pm 0.23 \times 10^{-4}$; plucked $-3.2 \pm 0.29 \times 10^{-4}$, $P < 0.02$ vs. control; trimmed $-2.5 \pm 0.54 \times 10^{-4}$, $P < 0.005$ vs. control). This reduction in peak strength suggests that whisker-evoked neural activity is reduced in D1 and D2 barrel columns following deprivation. Deprivation did not significantly alter peak WRA strength of any spared whisker versus controls (E1–2, C1–2, Table 1).

WRAs Shrink Uniformly with Deprivation

A major goal of this study was to determine whether deprivation-induced shrinkage of whisker representations is spatially isotropic or involves a preferential contraction away from neighboring spared or deprived whisker representations. Therefore, we quantitatively compared WRA shape in control and deprived rats. We first fit each WRA with an ellipse by calculating the first 2 principal components of the area enclosed by the -1.5×10^{-4} threshold. The eccentricity (elongation) of the ellipse was calculated as the ratio of the length of the smallest to largest principle components. WRAs were significantly elongated (noncircular) in control rats (mean eccentricity across all control WRAs, 0.40 ± 0.02 [$n = 72$]), with E-row whiskers having the most elongated WRAs and C-row whiskers having the least elongated WRAs (Table 1, and examples in Fig. 2). Neither D-row plucking nor trimming altered WRA eccentricity for D-row whiskers, relative to controls. Eccentricity of spared whisker WRAs was also unaffected, except for the C2 whisker in trimmed rats, which became modestly more circular with deprivation ($P < 0.04$) (Fig. 5 and Table 1).

A second measure of WRA shape is its "sharpness" from peak to outer contour (i.e., how rapidly intrinsic signal strength falls off spatially from the WRA peak). We defined WRA sharpness as the peak strength divided by the square root of the area enclosed by the -1.5×10^{-4} threshold. WRAs that did not exceed the -1.5×10^{-4} threshold were excluded from this calculation. We found that D-row deprivation increased WRA sharpness, with plucking significantly increasing sharpness of both D1 and D2 WRAs, and trimming significantly increasing sharpness of the D1 WRA (Fig. 5*B*). Deprivation did not change WRA sharpness for spared whiskers (not shown). This indicates that deprivation preferentially reduced intrinsic signal responses to deprived whiskers at the edge of the WRA (i.e., in surrounding columns) versus at the WRA center (in whisker's principal column).

Because deprived whisker WRAs both shrank and sharpened, we next tested whether shrinkage occurred preferentially from neighboring spared columns or deprived columns, or whether instead shrinkage was spatially uniform. In the D-row deprivation paradigm, neighboring barrel columns along a row (gamma, D1, D2, D3) are deprived, whereas neighboring columns along an arc (C- and E-row columns) are spared. We therefore tested whether deprived whisker WRAs preferentially shrank along arc or row axes. WRAs were aligned with barrel outlines from CO-stained, flattened tangential sections through S1 (see Methods, and see Fig. 2 for examples). The anatomical D-row axis was determined as the line through the centers of the D1 and D2 whisker barrels. We calculated the average intensity of all pixels within each WRA (bounded by the -1.5×10^{-4} contour) versus pixel position along the D-row axis, and along the orthogonal, within-arc axis, and fit these profiles with separate Gaussians. The ratio of the standard deviations of these Gaussians was used as an index of the relative elongation of the WRA along arc versus row axes. In control rats, D1 and D2 WRAs tended to be broader along the row versus the arc axis (mean arc/row width index: D1 0.89 ± 0.11; D2 0.79 ± 0.08; both significantly < 1.0, $P < 0.03$, *t*-test). If deprivation caused preferential contraction from spared whisker columns, the arc/row width index would have been expected to decrease. However, deprivation did not alter the arc/row width index for either D1 or D2 WRAs, indicating that WRA shrinkage was uniform in arc and row dimensions (Fig. 5*C*). Deprivation also did not alter the arc/row width index for any spared whisker WRA (data not shown).

A second test for differential shrinkage of WRAs in the arc versus row dimensions is to examine the orientation (rotation) of the elliptical fit of the WRA with respect to the within-row axis. In controls, WRAs tended to extend further along rows than along arcs (Figs 2, 3*B*), and as a result the long axis of the elliptical fit was usually well aligned with the anatomical D-row axis. If deprivation caused disproportionate shrinkage of the

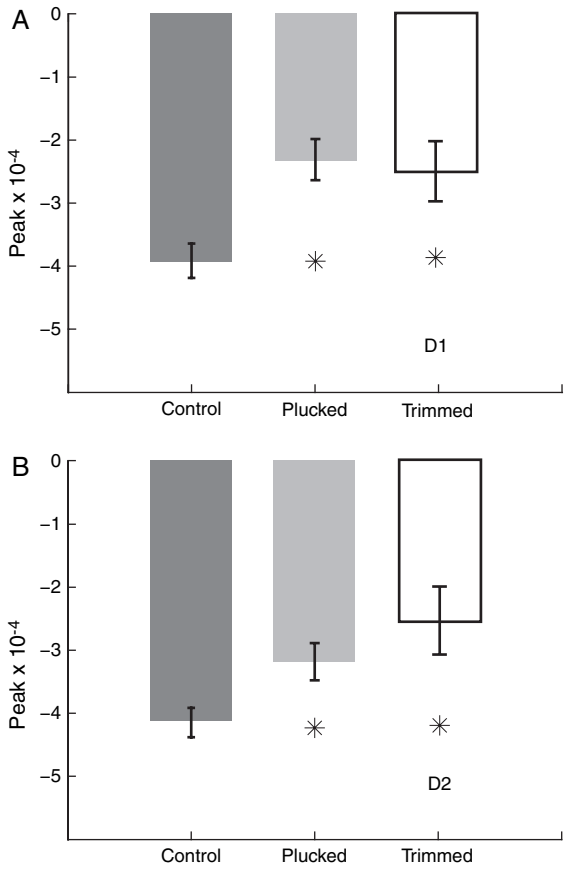

Figure 4. Effect of deprivation on peak magnitude of WRAs. (*A*) Average peak reflectance within the D1 WRA for control, D-row plucked and D-row trimmed animals. Asterisks denote significant differences ($P < 0.05$, 2-tailed *t*-test) from control animals. Reduced peak reflectance in D-deprived rats indicates reduced whisker-evoked neural activity. (*B*) Average peak reflectance for D2 WRAs. Conventions as in (*A*).

Table 1
WRA statistics for imaged whiskers

Whisker	Peak, -1×10^{-4}	Eccentricity	D-row projection/area$^{0.5}$	Angle relative to D axis mean ± dispersion (degrees)
C1	Control: 4.4 ± 0.35 (n = 12)	Control: 0.54 ± 0.05	Control: 0.68 ± 0.07	Control: 3.6 ± 22.9
	Plucked: 4.1 ± 0.26 (n = 11)	Plucked: 0.56 ± 0.06	Plucked: 0.69 ± 0.13	Plucked: 25.3 ± 27.1
	Trimmed: 4.0 ± 0.43 (n = 6)	Trimmed: 0.51 ± 0.05	Trimmed: 0.82 ± 0.14	Trimmed: 10.0 ± 7.9
C2	Control: 4.0 ± 0.34 (n = 10)	Control: 0.40 ± 0.05	Control: 0.75 ± 0.10	Control: 16.3 ± 15.7
	Plucked: 3.8 ± 0.32 (n = 5)	Plucked: 0.50 ± 0.05	Plucked: 0.52 ± 0.13	Plucked: −1.6 ± 70.0#
	Trimmed: 3.6 ± 0.54 (n = 6)	Trimmed: 0.63 ± 0.07*	Trimmed: 0.48 ± 0.23	Trimmed: 38.4 ± 35.9##
D1	Control: 3.9 ± 0.27 (n = 13)	Control: 0.45 ± 0.04	Control: 0.73 ± 0.07	Control: −17.2 ± 14.4
	Plucked: 2.3 ± 0.33* (n = 12)	Plucked: 0.37 ± 0.07	Plucked: 0.85 ± 0.24	Plucked: −17.0 ± 22.8
	Trimmed: 2.4 ± 0.48* (n = 7)	Trimmed: 0.33 ± 0.04	Trimmed: 0.90 ± 0.12	Trimmed: −4.9 ± 8.2
D2	Control: 4.1 ± 0.23 (n = 13)	Control: 0.41 ± 0.04	Control: 0.78 ± 0.06	Control: −24.0 ± 6.8
	Plucked: 3.2 ± 0.29* (n = 9)	Plucked: 0.46 ± 0.08	Plucked: 0.59 ± 0.15	Plucked: 17.2 ± 28.0##
	Trimmed: 2.5 ± 0.54* (n = 6)	Trimmed: 0.40 ± 0.08	Trimmed: 0.67 ± 0.09	Trimmed: −14.9 ± 2.2
E1	Control: 3.4 ± 0.31 (n = 13)	Control: 0.24 ± 0.02	Control: 1.05 ± 0.17	Control: −2.5 ± 25.9
	Plucked: 3.2 ± 0.30 (n = 10)	Plucked: 0.27 ± 0.03	Plucked: 0.93 ± 0.21	Plucked: 17.2 ± 44.0
	Trimmed: 3.7 ± 0.20 (n = 7)	Trimmed: 0.36 ± 0.02	Trimmed: 1.13 ± 0.13	Trimmed: −7.0 ± 0.7
E2	Control: 4.3 ± 0.33 (n = 11)	Control: 0.35 ± 0.05	Control: 0.95 ± 0.13	Control: −16.3 ± 9.6
	Plucked: 4.2 ± 0.90 (n = 8)	Plucked: 0.34 ± 0.04	Plucked: 0.62 ± 0.13	Plucked: −1.7 ± 48.3##
	Trimmed: 3.7 ± 1.13 (n = 6)	Trimmed: 0.38 ± 0.06	Trimmed: 0.65 ± 0.11	Trimmed: −17.3 ± 10.7

Note: *$P < 0.05$, #$P < 0.05$, **$P < 0.01$, ##$P < 0.01$.

WRA along one axis (e.g., the arc axis), then the major elliptical axis of the WRA should rotate away from that axis. To test this, we quantified the angular difference between the long axis of the ellipse and the D-row axis. Positive angles mean counterclockwise rotation of the ellipse long axis relative to the anatomical D-row axis. We found no significant change in this angle for plucking or trimming the D1 whisker, and no consistent changes for the D2 whisker (Table 1). For spared whiskers, occasional significant differences were found, but these were not in a consistent direction (Bootstrap test, Table 1).

As a final test for differential shrinkage along arc versus row dimensions, we calculated an index that represents the relative extent of the WRA along the D-row axis, based on the elliptical fit to the WRA. This index was obtained by projecting the long axis of the ellipse onto the anatomical D-row axis (determined from CO-stained sections), and calculating the length of this projection divided by the square root of the WRA area. If deprivation shrank WRAs isotropically, this index should remain constant. If deprivation preferentially shrank WRAs in the row dimension, then this ratio should decrease. We found no significant change in this index for any whisker, with plucking or trimming (Fig. 5*C*, Table 1).

Together, these findings indicate that D-row deprivation weakens and shrinks deprived whisker WRAs, and makes them spatially sharper. However, this shrinkage occurred in a spatially uniform manner, without altering the eccentricity of the WRA or its relative spread along arc versus row axes.

Position of WRAs Relative to the Anatomical Barrel Map

We next asked how well the WRAs were aligned with the anatomical barrel map, as determined from CO-stained sections, and whether this alignment was perturbed by deprivation. We measured the distance from the geometrical center of each WRA (derived from the -1.5×10^{-4} contour) to the center of the corresponding anatomical barrel from aligned, CO-stained sections through layer 4 (Fox 1992). Across all imaged barrels (n = 145), the mean of the magnitude of the absolute distance from WRA center to barrel center was 252 ± 16 μm (median 209 μm). There was no clear trend in direction of error.

We first tested whether deprivation caused WRAs of C- and E-row whiskers to shift toward the deprived D-row, as can occur with prolonged periods of deprivation (Kossut 1989). We found that for spared whiskers, the mean distance from the geometrical center of each WRA to the center of its corresponding anatomical barrel did not change significantly (C1: control 356 ± 74 μm; plucked 222 ± 63; trimmed 137 ± 24; C2: control 374 ± 102 μm, plucked 222 ±34, trimmed 125 ± 41; E1: control 254 ± 61 μm; trimmed 281 ± 52; plucked 279 ± 77; E2: control 281 ± 65 μm; trimmed 286 ± 69; plucked 358 ± 40). Across all whiskers in plucked and trimmed rats, the absolute value of the distance from WRA center to barrel center was 227 ± 20 μm (median 203 μm). There were no significant differences or clearly observable trend in direction of spatial error between WRA and anatomical barrels for control versus deprived animals (multivariate ANOVA) (Fig. 6*A*).

To further test whether deprivation caused WRA centers to shift relative to each other, we measured the distance between C1, D1, and E1 WRA centers, and between C2, D2, and E2 WRA centers in control, plucked, and trimmed rats. We found no significant difference in these dimensions (C1–E1: control 0.97 ± 0.05 mm, plucked 0.94 ± 0.07, $P < 0.89$; trimmed 1.01 ± 0.06, $P < 0.52$; C2–E2: control 0.86 ± 0.05 mm, plucked 0.87 ± 0.12, $P < 0.80$; trimmed 0.94 ± 0.04, $P < 0.52$; C1–D1: control 0.53 ± 0.04 mm, plucked 0.41 ± 0.04, $P < 0.83$; trimmed 0.51 ± 0.04, $P < 0.83$; D2–C2: control 0.41 ± 0.20 mm; plucked 0.45 ± 0.10, $P < 0.68$; trimmed 0.57 ± 0.08, $P < 0.19$; D1–E1: control 0.49 ± 0.03 mm; plucked 0.55 ± 0.09, $P < 0.45$; trimmed 0.50 ± 0.05, $P < 0.62$; D2–E2: control 0.51 ± 0.05 mm; plucked 0.56 ± 0.09, $P < 0.84$; trimmed 0.51 ± 0.12, $P < 0.066$) except for D1–C1 distance, which decreased in plucked rats (control 0.53 ± 0.04, plucked 0.41 ± 0.04, $P < 0.05$). These findings show that deprivation did not systematically alter the relative locations of WRAs or their positions relative to the anatomical barrel map.

We summarize how deprivation altered the WRA map in Figure 6*B*. This figure plots the mean elliptical fit for each whisker's WRA (averaged across rats), and the relative spacing between WRA centers, averaged across the population. Crosses indicate the mean location of the anatomical barrel columns. This summary shows that D-row trimming and plucking shrank the D1 and D2 WRAs, without significantly altering their shape or orientation. Spared whisker WRAs were largely unaffected

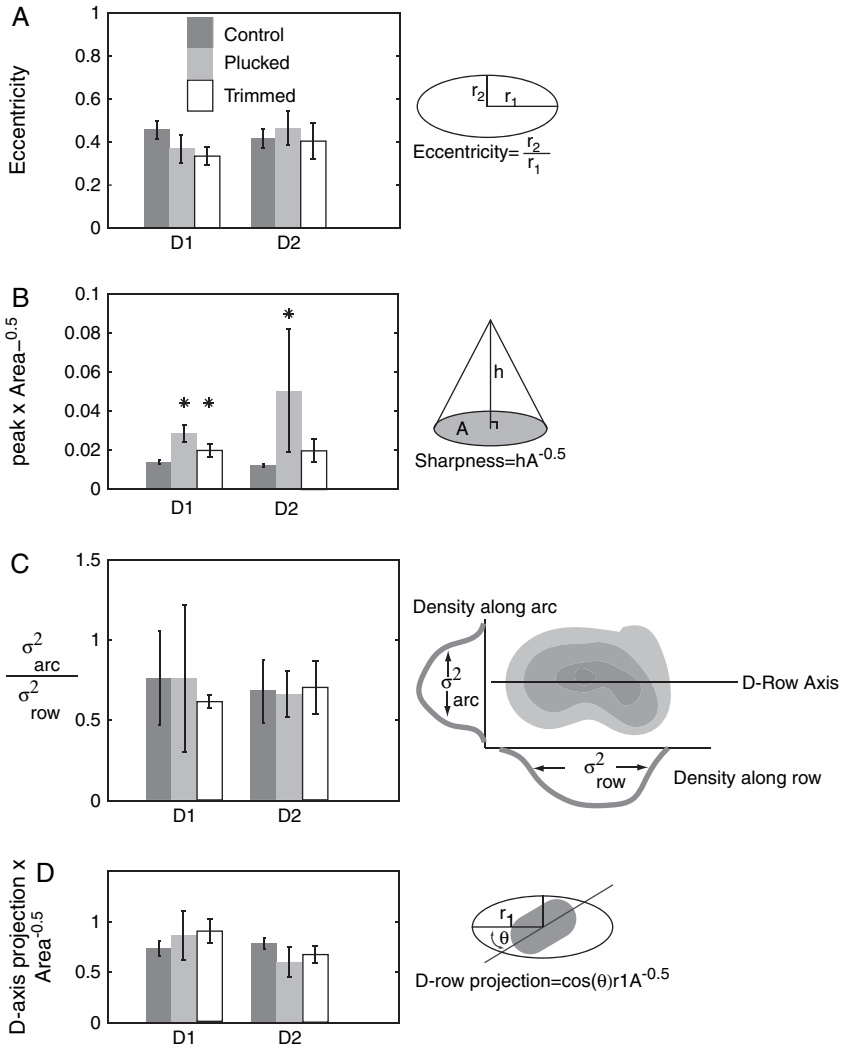

Figure 5. Effects of deprivation on shape of deprived WRAs. (*A*) Eccentricity of D1 (left) and D2 (right) WRAs. Eccentricity is the ratio of smallest to largest principle components, with 0 corresponding to a line, and 1 to a circle. There are no significant differences between the control D1 and D2 WRAs and the plucked and trimmed WRAs. (*B*) Ratio of the WRA peak to the square root of the area within the -1.5×10^{-4} threshold. An increase in this ratio implies a "steepening" of the WRA. There is a significant increase in this ratio relative to controls in plucked D1 and D2 WRAs, and in trimmed D1 WRAs. There were no significant changes in the spared WRAs relative to controls (not shown). (*C*) Ratio of the projection of the inner product of the anatomically determined D-row axis and the long axis of the WRA eccentricity to the square root of area. A decrease in this ratio implied that there is disproportionally more shrinkage along the D-row axis. There is no significant difference between control and deprived D-row WRAs. (*D*) Ratio of the spread of the WRA along the arc axis to the spread along the row axis. Increase indicates more contraction along the row than the arcs. There is no significant change in this ratio between control and D-row plucked and trimmed WRAs in the D-row or for other WRAs (data not shown). (*E*) Difference between the angle of the largest principal component of the D1 (left) and D2 (right) WRAs and the axis of the D-row determined from layer 4 CO staining for control, plucked, and trimmed animals.

by deprivation, except for the E2 WRA, which shrank during trimming for unknown reasons (Fig. 3*A*).

Single-Unit Electrophysiological Recordings

We verified these deprivation-induced changes in the whisker map using electrophysiological recordings (7 control, 6 D-row plucked, 1 D-row trimmed). Data from plucked and trimmed rats were combined. One hundred and ninety-three single-unit recordings were obtained from layers (L) 2/3 and 4 of D1, D2, and E1 barrel columns. Penetrations were targeted using WRAs from intrinsic imaging, and recording position was verified in all cases by histological recovery of marking lesions in CO-stained tangential sections through L4 (Fox 1992). Recording penetrations through L4 septa were excluded. Single-unit selection criteria were identical in control vs. deprived animals, as were spontaneous firing rates in D columns (L2/3, control vs. deprived, $P < 0.60$; L4, $P < 0.91$) and E columns (L2/3: $P < 0.57$; L4: $P < 0.12$) (see Table 2), suggesting that unit selection bias was similar in both conditions. For each unit, responses were measured to randomly interleaved deflections of 9 adjacent whiskers, centered around the anatomically appropriate whisker for the recording column.

Figure 7 shows representative single-unit recordings from L2/3 of the D1 column in a control rat and a D-row plucked rat. Recording penetrations (denoted by *x*'s in Fig. 7*A*, *D*) were confirmed to be within the anatomical D1 barrel column (black outline), based on recovery of marking lesions, and were located near the center of the D1 WRA in each case (contours in Fig. 7*A*, *D*). Spike waveform density plot and ISI histogram (all ISI > 2 ms) demonstrate single-unit isolation (Fig. 7*B*, *E*). Both units responded most strongly to D1 whisker deflection, consistent with D1 column location (Fig. 7*C*, *F*). However,

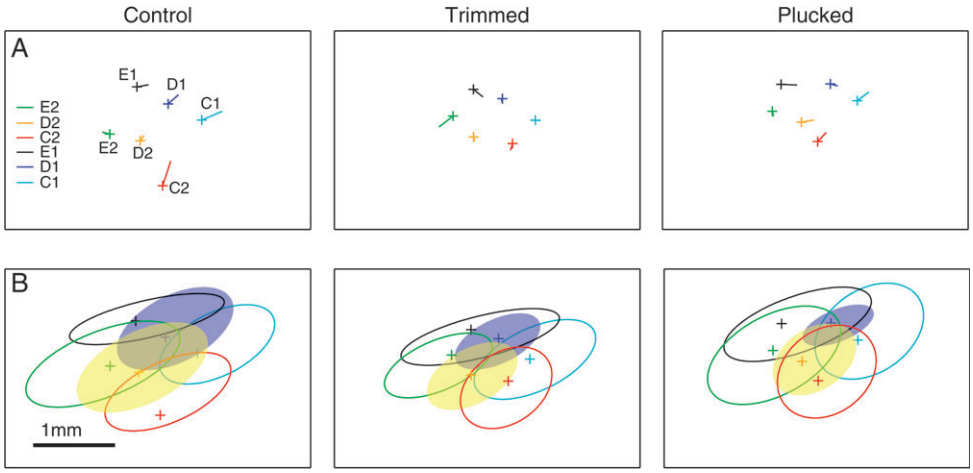

Figure 6. Effects of deprivation on position of WRAs. (*A*) Error between center of the -1.5×10^{-4} contour and center of anatomically defined barrel. Crosses show barrel centers, lines from centers show direction and magnitude of the mismatch between anatomy and imaging. (*B*) Average WRAs represented by ellipsoids with average area and eccentricity of WRAs. Crosses show location of barrels centers. Left, average of control animals, center, trimmed animals, and right, plucked animals. The 3 conditions have similar average maps, except for the shrinkage of the D-row WRAs in the deprived row.

Table 2
Single-unit responses to principal whisker deflection in D-row barrel (D1 + D2) columns

All are means ± SE except latency, median ± SE	Layer 2/3 deprived (n = 35)	Layer 2/3 control (n = 47)	Layer 4 deprived (n = 20)	Layer 4 control (n = 32)
Spontaneous rate, spikes/s	1.51 ± 0.24 ($P < 0.85$)	1.50 ± 0.23	2.62 ± 0.48 ($P < 0.21$)	2.75 ± 0.71
On rate, spikes/s (5–25 ms after whisker deflection)	24.12 ± 3.623** ($P < 5.2 \times 10^{-5}$)	61.79 ± 7.12	40.26 ± 8.90* ($P < 0.016$)	64.45 ± 7.22
Tonic rate, spikes/s (25–105 ms after whisker deflection)	7.67 ± 1.20** ($P < 0.0017$)	5.55 ± 1.42	5.53 ± 1.25* ($P < 0.023$)	3.18 ± 1.10
Off rate, spikes/s (105–125 ms after whisker deflection)	24.29 ± 3.06** ($P < 2.3 \times 10^{-5}$)	56.99 ± 7.17	51.35 ± 9.45 ($P < 0.15$)	66.83 ± 7.82
Total rate, spikes/s	12.43 ± 1.48** ($P < 0.005$)	25.15 ± 3.02	15.76 ± 3.78 ($P < 0.18$)	22.27 ± 5.07
Latency (median), ms	14.5 ± 9.11** ($P < 8.4 \times 10^{-6}$)	12 ± 3.03	11 ± 1.11 ($P < 0.10$)	12 ± 5.37

Note: *$P < 0.05$; **$P < 0.01$.

Table 3
Single-unit responses to E1 whisker deflection in the E1 barrel column

All are means ± SE, except latency, median ± SE	Layer 2/3 deprived (n = 13)	Layer 2/3 control (n = 24)	Layer 4 deprived (n = 11)	Layer 4 control (n = 11)
Spontaneous rate, spikes/s	0.87 ± 0.13 ($P < 0.43$)	1.2 ± 0.30	2.34 ± 0.44 ($P < 0.09$)	1.26 ± 0.19
On rate, spikes/s (5–25 ms after whisker deflection)	30.06 ± 5.59 ($P < 0.58$)	35.14 ± 4.63	68.19 ± 12.54 ($P < 0.56$)	49.98 ± 10.72
Tonic rate, spikes/s (25–105 ms after whisker deflection)	7.69 ± 1.91 ($P < 0.14$)	4.86 ± 0.99	3.48 ± 1.64 ($P < 0.51$)	4.5 ± 1.35
Off rate, spikes/s (105–125 ms after whisker deflection)	25.89 ± 5.07 ($P < 0.38$)	43.87 ± 9.36	63.40 ± 11.12 ($P < 0.57$)	80.37 ± 17.77
Total rate, spikes/s	13.87 ± 2.18 ($P < 0.54$)	16.17 ± 1.95	25.73 ± 4.26 ($P < 0.55$)	22.31 ± 4.07
Latency, ms	14 ± 0.94 ($P < 0.19$)	12 ± 0.62	10 ± 0.24 ($P < 0.007$)*	12 ± 0.99
Total response to D1 deflection, spikes/s	0.78 ± 0.53 Hz ($P < 0.0001$)**	5.19 ± 0.79	1.99 ± 0.84 Hz, ($P = 0.03$)*	6.28 ± 2.01 Hz

Note: *$P < 0.05$; **$P < 0.01$.

responses to deprived whiskers (D1, D2, and delta) were substantially weaker in the deprived rat than the control rat.

This effect was consistently observed across L2/3 single units in D columns of D-row deprived versus control rats. We first visualized the mean effect of deprivation across the population of L2/3 single units by calculating mean population PSTHs for all single units in specific cortical columns (Fig. 8). In control rats, units in L2/3 of the D1 column (penetration locations shown in Fig. 8*A*) responded best, on average, to the D1 whisker, with smaller but substantial responses to the immediately surrounding D2, delta, gamma, E1, and C1 whiskers (Fig. 8*B*). Deprivation of the D-row of whiskers (including gamma, D1, and D2) substantially reduced mean neural responses to these deprived whiskers measured in the D1 column, but left mean responses to spared C-row whiskers largely unchanged (control: n = 47 units; deprived: n = 26 units). D-row deprivation also reduced responses to spared E1 and delta whisker in the D1 column (consistent with Wallace and Sakmann 2007; see Discussion). In L2/3 of the E1 column (Fig. 8*C*), responses to E-row whiskers (delta, E1, E2) were not substantially affected by D-row deprivation; however, deprivation virtually eliminated responses to the D1 whisker (control: n = 24 units; deprived: n = 13 units) (Fig. 8*C*). Thus, D-row deprivation weakened responses to D-row whiskers, without driving strengthening or expansion of spared C- and E-row whisker responses.

Depression of D-Row Whisker Responses in Home Columns

To quantify the effects of D-row deprivation on single-unit responses, we first examined how deprivation altered

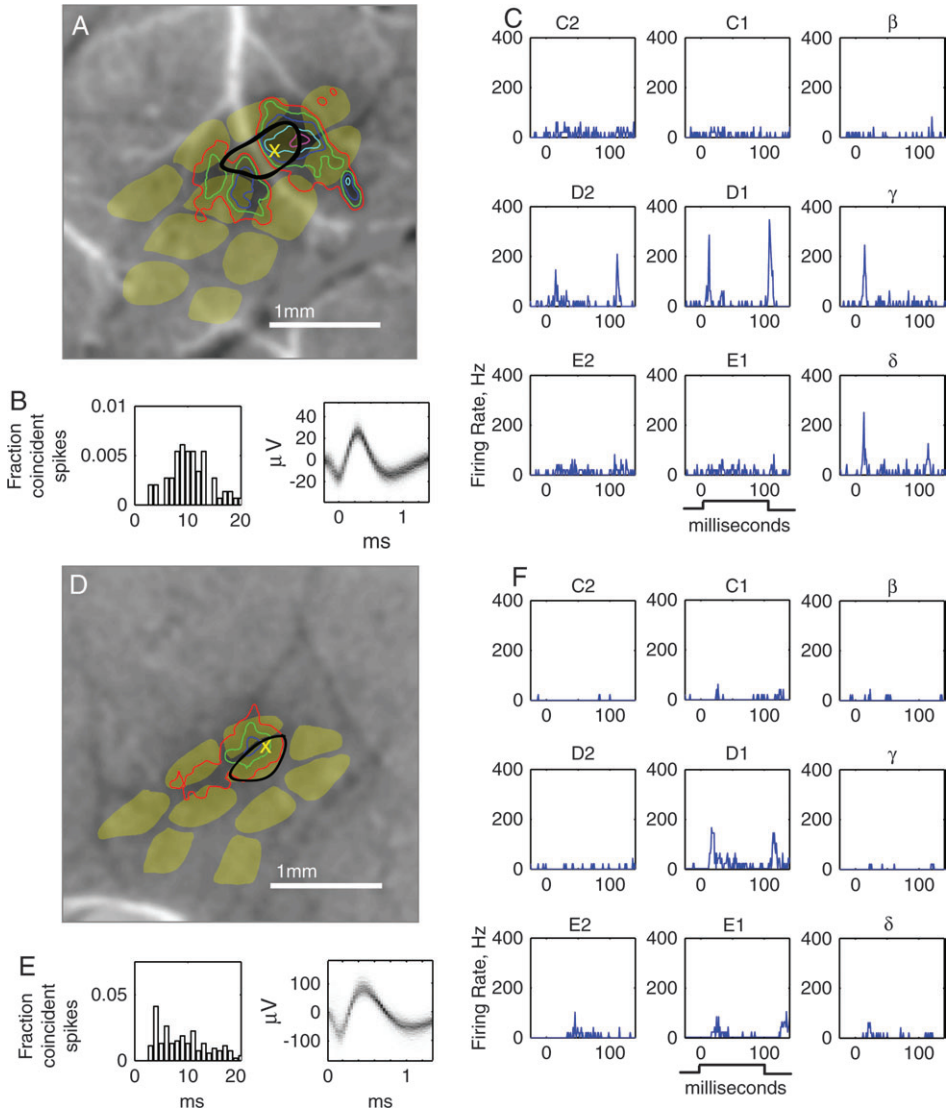

Figure 7. Representative single-unit recordings in L2/3 of the D1 column in control and deprived rats. (*A–C*) L2/3 single unit in the D1 column of a control rat (depth: 586 μm below the pia). (*D–F*) L2/3 single unit in the D1 column of a D-row plucked rat (depth: 512 μm below pia). (*A*, *D*) Location of recording sites (X) relative to barrel outlines from CO-stained sections, and to D1 WRA used to target the recording penetration (contours, same thresholds as in Fig. 2). Background, D1-evoked intrinsic signal image. (*B*, *E*) Single-unit isolation shown by ISI histogram (left) and spike waveform density plot (right). (*C*, *F*) Nine-whisker tuning curve showing responses to 100-ms ramp–hold–return deflections (deflection onset: 0 ms). On- and off-responses are clearly visible. Each PSTH is mean of 50 sweeps.

responses to D-row whiskers within their anatomical home columns (Fig. 9). (The home column corresponds to the central ~400 μm of the WRA). Data were combined across recordings in both the D1 column (responses to the D1 whisker) and the D2 column (responses to the D2 whisker). L2/3 and L4 units were analyzed separately. Intrinsic signal maps are likely to primarily reflect neural activity in L2/3. For L2/3 single units (recording locations in Fig. 9*A*, left), D-row deprivation caused pronounced depression of responses to deprived D1 and D2 principal whiskers. This was evident in the mean population PSTH (Fig. 9*B*, left; control: n = 47 units; deprived: n = 35 units; these data include the D1 recording sites from Fig. 8*B*). Background (spontaneous) firing rate was unaffected (Fig. 9*C*, left). Deprivation dramatically reduced ON-responses, defined as spikes occurring 5–25 ms after deflection onset (Fig. 9*D*, left), from 61.8 ± 7.1 Hz in control rats to 24.1 ± 3.6 Hz in deprived rats, a reduction of 61%. Deprivation also reduced OFF-responses (Table 2). Total responses (5–130 ms after deflection onset) were reduced from 25.1 ± 3.0 Hz in control rats to 12.4 ± 1.5 Hz in deprived rats, a reduction of 50% (Fig. 9*E*, left). This decreased whisker response was accompanied by a significant increase in onset latency (Fig. 9*F*, left; P = 0.002, Mann–Whitney test). Reduced principal whisker responses were not artifact of differential sampling of recording locations within D1 and D2 barrel columns (Armstrong-James and Fox 1987), because identical effects were observed when analysis was restricted to recording sites in the central 50% of the barrel column, measured along the arc axis (ON-responses for L2/3 single units: control: 63.0 ± 8.0 Hz, n = 41; deprived: 20.1 ± 4.3 Hz, n = 26, P < 0.00004).

In contrast, deprivation slightly increased sustained (tonic) responses (25–105 ms after deflection onset, prior to return deflection) from 5.6 ± 1.4 Hz in control rats to 7.7 ± 1.2 Hz in deprived rats (Table 2). This effect was particularly evident late

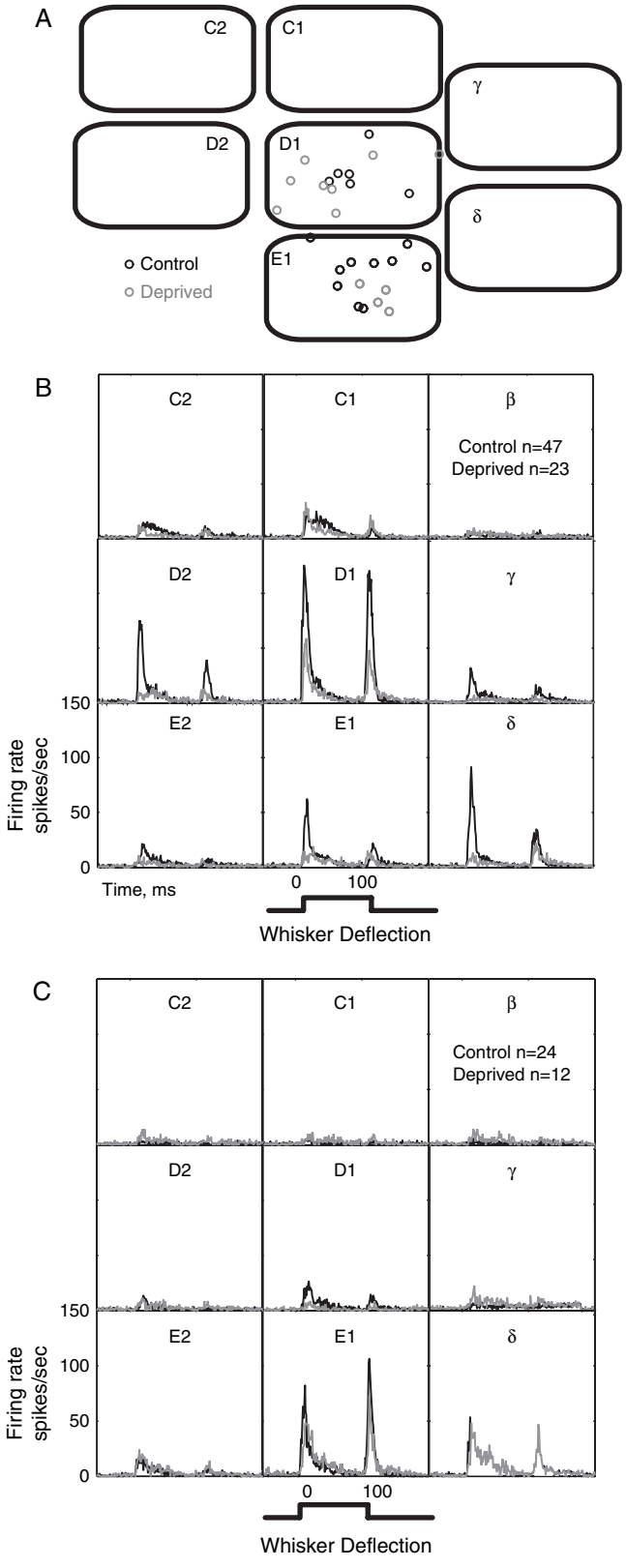

Figure 8. Effect of deprivation on population average whisker responses in D1 and E1 columns. (*A*) Location of all recording penetrations in D1 and E1 columns in control ($n = 7$) and D-row deprived ($n = 6$) rats, relative to normalized anatomical barrel boundaries. (*B*) Population average PSTHs for whisker responses of all single units recorded in L2/3 of the D1 whisker column. Instantaneous firing rate is calculated for each 1-ms time bin. Black, control rats. Gray, deprived rats. (*C*) Population average PSTHs for whisker responses for all single units recorded in L2/3 of the E1 whisker column.

in the sustained response (55–105 ms: control, 0.14 ± 0.57 Hz; deprived, 4.9 ± 1.0 Hz, $P < 0.0006$), indicating that it was not due to the slight increase in latency of deprived responses. Because sustained responses are normally minimized by inhibition (Foeller and Feldman 2005), the increased in sustained responses suggests that deprivation may decrease inhibition.

In L4, unlike L2/3, deprivation caused only a modest depression of deprived principal whisker responses (Fig. 9, right column). A modest reduction in ON-responses is apparent in the population PSTH (Fig. 9*B*, right). This reduction was significant (Fig. 9*D*) (control ON response: 64.5 ± 7.2 Hz, $n = 32$ units; deprived: 40.3 ± 8.9 Hz, $n = 20$ units, a reduction of 38%, $P < 0.02$). However, OFF-responses were not significantly reduced (control: 66.8 ± 7.8 Hz; deprived: 51.4 ± 9.5 Hz, $P = 0.15$, Table 2), and sustained responses were modestly increased (Table 2). As a result, total responses showed a nonsignificant decrease (Fig. 9*E*) (control: 22.3 ± 5.1 Hz, deprived: 15.8 ± 3.8 Hz, $P < 0.18$, this represents a 29% numerical decrease, compared with a 50% decrease in L2/3). Neither background firing rate nor principal whisker response latency was changed (Fig. 9*C*, *F*). Together, these findings indicate that deprivation modestly weakened early L4 responses to deprived whiskers, but that this weakening was much smaller than in L2/3. Weakening was most prominent for the earliest whisker responses in L4 (5–10 ms after deflection onset; control: 48.8 ± 8.14 Hz; deprived: 20.66 ± 5.35 Hz; $P < 0.02$), suggesting that deprivation may weaken thalamocortical input to L4 (SupplementaryFig. 2).

Depression of D-Row Whisker Responses in Surrounding Columns

We next quantified how deprivation affected responses to deprived D-row whiskers measured in cortical columns surrounding the home column (Fig. 10). A strong reduction in D-row whisker responses would be expected in these surround columns, which correspond to the edges of the D-row whisker WRA defined by intrinsic signal imaging.

First, we analyzed responses to the deprived D1 whisker by single units in the spared surrounding E1 column (recording site locations shown in Fig. 8*A*). Deprivation reduced total responses of L2/3 single units from 5.19 ± 0.79 Hz (control, $n = 24$ units) to 0.78 ± 0.53 Hz (deprived, $n = 13$ units), a reduction of 84% ($P = 0.0001$) (Fig. 10*A*, left). Single-unit responses in L4 were reduced more modestly, but still significantly (control: 6.28 ± 2.01 Hz, deprived: 1.99 ± 0.84 Hz, $P = 0.03$) (Fig. 10*A*, right).

Next, we analyzed responses to deprived D-row whiskers in surrounding deprived columns. Because most of our recording sites were in the D1 column, we did this by calculating the mean response to D2 and gamma whiskers (both of which were deprived) at recording sites in the D1 column (which was also deprived). In control rats, the mean response to D2 and gamma whiskers by single L2/3 units in the D1 column was 10.28 ± 1.07 Hz ($n = 47$ units). This was reduced by D-row deprivation to 5.25 ± 1.07 Hz ($n = 26$ units), a reduction of 60% (Fig. 10*B*, left). This reduction was significant ($P < 0.00001$). Single-unit responses in L4 were reduced slightly, but not significantly (control: 8.34 ± 1.18 Hz, deprived: 7.85 ± 2.31 Hz, $P > 0.05$) (Fig. 10*B*, right).

These effects of D-row deprivation on the cortical representation of D-row whiskers are summarized in Figure 10*C*. In

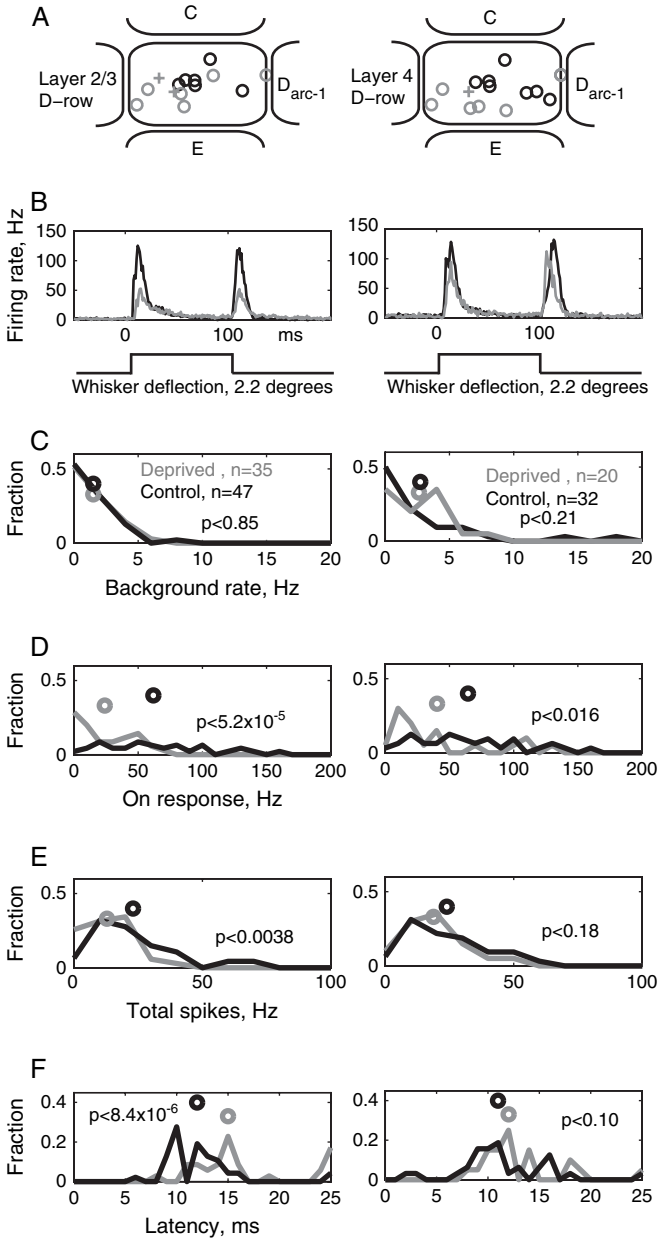

Figure 9. Single-unit responses to deprived D1 and D2 whiskers measured in their home columns. (*A*) Location of all recording penetrations in D1 and D2 columns in control ($n = 7$) and deprived ($n = 7$) rats, relative to normalized column boundaries. Circles, D1 penetrations; +, D2 penetrations. Black, control cases. Gray, deprived cases. (*B*) Population average PSTHs of principal whisker responses, for all L2/3 (left) and L4 (right) units, in D1 and D2 columns. The left column includes data for units in D1 columns from Figure 8*B*. (*C*) Spontaneous firing rate distribution and means. (*D*) Magnitude of ON response (5–25 ms after onset of whisker deflection) to principal whisker deflection. Circles show mean. (*E*) Magnitude of total response to principal whisker deflection (5–130 ms after deflection onset). (*F*) Onset latency of principal whisker responses for all single units in D1 and D2 columns. Circles, median latency. All statistics are results of Mann–Whitney *U* test.

L2/3, D-row deprivation reduced single-unit spiking responses to the deprived D1 whisker, within its own home column, by 50%. Deprivation reduced responses to deprived whiskers in surrounding columns slightly more: by 60% in surrounding deprived columns, and by 84% in surrounding spared columns (Fig. 10*C*, left). Smaller reductions occurred in L4 (Fig. 10*C*, right). Thus, deprivation weakened responses to deprived whiskers more strongly in surrounding columns than in the whisker's home column, consistent with the sharpening of the WRA observed with intrinsic signal imaging.

Single-Unit Responses to Spared Whiskers

Finally, we analyzed the effects of D-row deprivation on single-unit responses to spared whiskers, whose representations appeared largely unchanged by intrinsic signal imaging (Fig. 11). We first focused on responses to E1 whisker deflection within its home, E1 column. ON-responses to E1 whisker deflection in the E1 column were unchanged by D-row deprivation, both for L2/3 single units (Fig. 11*A*, left) and L4 single units (Fig. 11*A*, right). Background firing rate and total responses to E1 whisker deflection were similarly unchanged (Fig. 11*B*, *C*). To determine whether responses to spared E-row whiskers were altered within deprived (D-row) columns, we examined responses to E1 whisker deflection measured in the D1 column. Deprivation caused a significant reduction of total responses to the E1 whisker within the D1 column in L2/3 (Fig. 11*D*, left) (control: 7.78 ± 1.27 Hz, deprived: 4.55 ± 0.92 Hz; $P < 0.006$), consistent with the population PSTH data shown in Figure 8*B*. Deprivation paradoxically increased these responses in L4 (control: 5.57 ± 1.16 Hz, deprived: 7.78 ± 1.27 Hz; $P < 0.04$) (Fig. 11*D*, right). However, responses to C1 were unchanged in L2/3 of the D1 column (control: 10.42 ± 1.72 Hz; deprived: 13.03 ± 3.81 Hz, $P < 0.68$). Thus, 1) deprivation did not alter spared whisker responses within their home columns; 2) spared whisker responses did not significantly expand into deprived columns; and 3) there was mixed evidence for withdrawal of spared whisker responses from deprived columns, with some whiskers showing such withdrawal, but others not.

Discussion

Deprivation of a subset of whiskers classically drives 2 components of map plasticity: rapid weakening/contraction of deprived sensory representations, and a slower strengthening/expansion of spared sensory representations (Fox 2002; Feldman and Brecht 2005). The present study characterizes the first component of plasticity, which is particularly prominent in the first postnatal weeks and months (Fox 2002). Results showed that D-row deprivation for 6–10 days, beginning at P20, reduced the functional representation of deprived whiskers, measured by both intrinsic signal imaging and single-unit electrophysiology. In contrast, the representation of spared whiskers did not change. Thus, this deprivation protocol selectively engages the rapid depression component of plasticity, at least in L2/3 and L4, where measurements were made.

A primary goal of this study was to spatially characterize the weakening/contraction of deprived whisker representations, in order to infer the learning rules and sites of plasticity that may be involved (see below). Intrinsic imaging revealed that deprivation reduced the peak amplitude and spatial extent of deprived whisker representations, with greater suppression of responses at the edges of the WRA than in its center (Figs 3–5). Correspondingly, single-unit responses to deprived whiskers decreased significantly in L2/3 of the home column, and decreased even more sharply in neighboring columns (Fig. 10*C*). Analysis of the shape of WRAs showed that contraction was spatially uniform, with deprived whisker WRAs shrinking

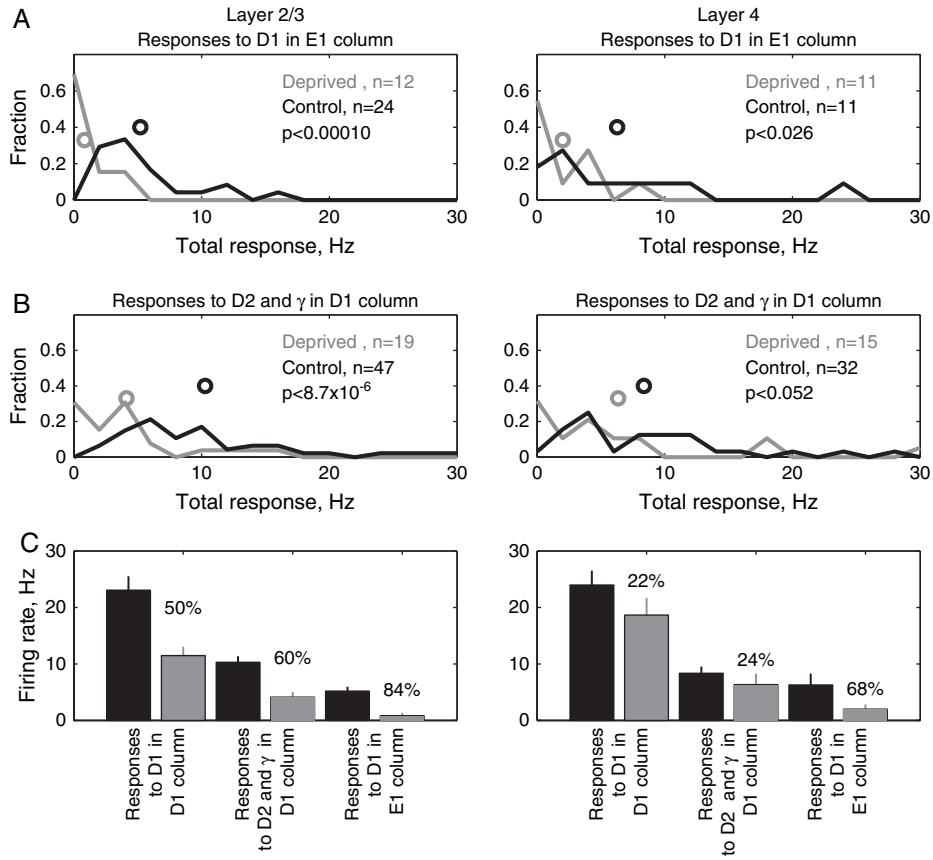

Figure 10. Single-unit responses to deprived whiskers measured in surrounding columns. (*A*) Total responses to the D1 whisker measured for single units in the E1 column. Recording penetration locations are shown as circles in the E1 column in Figure 8A. ON-responses (5–25 ms after deflection onset) to the E1 whisker measured for single units in the E1 column. Recording penetration locations are shown as circles in the E1 column in Figure 8*A*. (*B*) Total responses to D2 and gamma whiskers in D1 column. (*C*) Mean total response magnitude for deprived D1, D2, and gamma whiskers in different cortical columns. Left, response to D1 whisker in its home, D1 column (from Fig. 9). Middle, mean response to D2 and gamma whiskers in the deprived D1 column. Right, response to D1 whisker in the spared E1 column. Percentages represent the magnitude of response reduction in deprived animals, relative to the control animals.

equally from neighboring spared and deprived columns. This isotropic contraction contrasts with the effects of deprivation on spared whisker representations, which expand preferentially into neighboring spared columns (Diamond et al. 1993, 1994; Armstrong-James et al. 1994; Lebedev et al. 2000), and/or withdraw preferentially from deprived columns (Wallace and Sakmann 2007), depending on age and measurement technique. Thus, contraction of deprived whisker representations occurs with a distinct spatial profile relative to expansion of spared whisker representations. This suggests that these 2 components of plasticity may involve distinct synaptic loci and/or learning rules for plasticity.

When deprivation is performed by whisker plucking, cortical responses are evoked by deflecting the regrowing whisker, which is thin and mechanically compliant. Thus, a major concern is to ensure that the deprivation-induced reduction in whisker responses is not due, trivially, to an inability of the partially regrown whisker to transmit vibrations to the follicle. We addressed this by comparing the effects of D-row whisker plucking with D-row whisker trimming on intrinsic signal maps. (In D-row trimming, cortical responses were measured by deflecting the whisker stub, which is of normal diameter and mechanical stiffness.) D-row trimming weakened deprived whisker representations in intrinsic imaging maps identically to D-row plucking, indicating that the loss of responses to deprived whiskers is not due to failure to mechanically stimulate the whisker follicle (Figs 3–5). This is consistent with prior studies showing that whiskers partially regrown after plucking evoke normal spiking responses in thalamus and L4 of S1 (Glazewski and Fox 1996; Glazewski et al. 1998; Foeller and Feldman 2005).

Utility and Interpretation of Intrinsic Imaging for Assaying Map Plasticity

Compared with traditional electrophysiological mapping procedures that use discrete electrode penetrations, optical imaging samples map topography in a fine-grained, spatially continuous manner, thus allowing direct visualization of the spatial profile of map plasticity. Intrinsic signal imaging has been used extensively to study V1 map plasticity (e.g., Crair et al. 1997a, 1997b; Sengpiel et al. 1998; Cang et al. 2005; Smith and Trachtenberg 2007). In S1, intrinsic imaging and voltage-sensitive dye imaging have been used to measure plasticity of spared whisker representations (Polley et al. 1999; Wallace and Sakmann 2007), but plasticity of deprived whisker representations has not previously been examined.

Two critical issues are the nature of the neural signal that is reported by intrinsic signal imaging, and the spatial resolution of this technique. Intrinsic imaging measures hemodynamic changes in blood oxygenation and metabolic activity due to local neural activity, and thus reflect both the spatial extent of

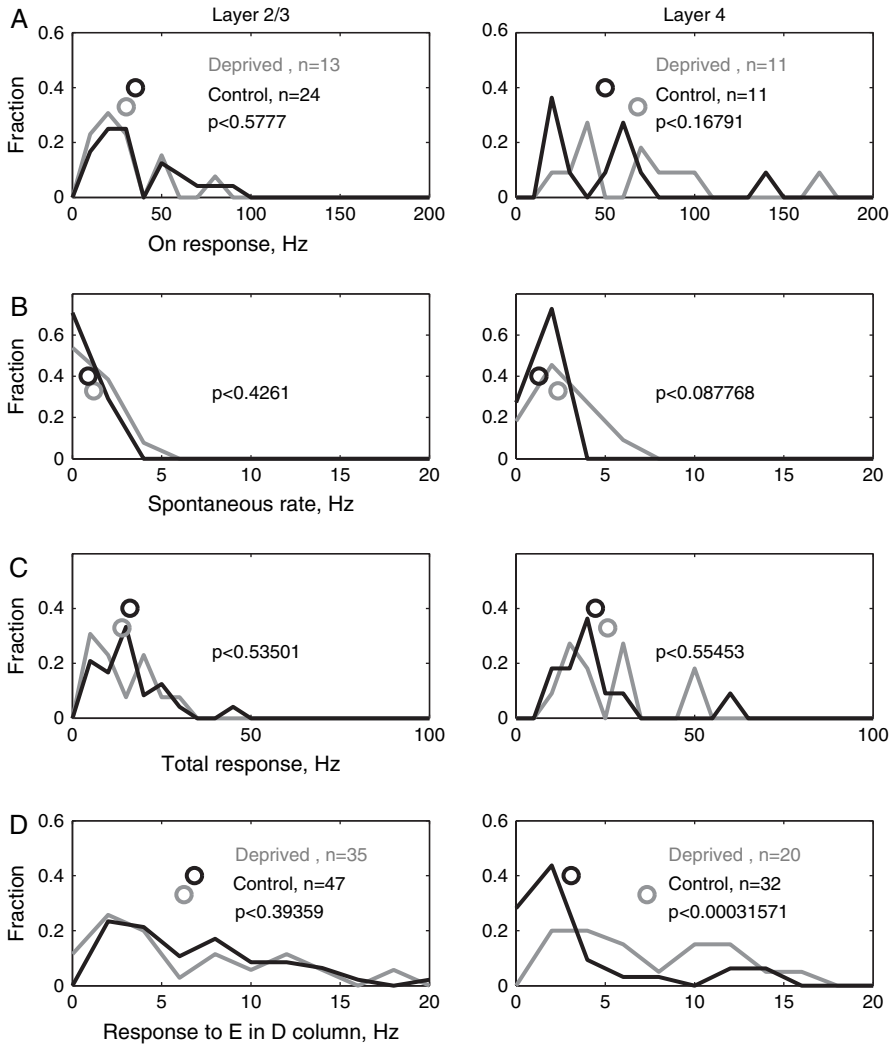

Figure 11. Single-unit responses to the spared E1 whisker. (*A*) ON-responses to the E1 whisker measured for single units in the E1 column. Recording penetration locations are shown as circles in the E1 column in Figure 8*A*. (*B*) Spontaneous firing rate for single units in the E1 column. (*C*) Total responses (5–130 ms after deflection onset) to E1 deflection for single units in the E1 column. (*D*) Total responses to E1 whisker deflection for single units in the D1 column). Recording site locations are shown in Figure 8*A* (D1 sites).

neural activity and the spatial resolution of neurovascular coupling (Masino et al. 1993). In S1, the magnitude and spatial profile of intrinsic signal (and particularly, the initial dip in reflectance) correlates well with neuronal spiking responses, suggesting that it primarily reflects suprathreshold cortical responses (Petersen et al. 1998; Masino 2003). In this interpretation, the fact that WRAs are large (~1 mm^2) compared with anatomical whisker columns (~0.25 mm^2), reflects the fact that whisker deflection evokes spikes both in the whisker's home column, and, to a lesser extent, in surround columns (Simons 1978; Armstrong-James and Fox 1987). However, intrinsic signal may also reflect subthreshold activity and/or glutamate release and astrocytic uptake (Nemoto et al. 2004; Gurden et al. 2006), which have a greater spatial extent than spiking responses (e.g., Moore and Nelson 1998; Brecht et al. 2003).

Three observations suggest that the spatial resolution of intrinsic signal imaging is sufficient to have detected anisotropic shrinkage of deprived whisker WRAs. First, anisotropic changes in spared whisker representations occur over a relatively large, 0.5–1 mm spatial scale during a similar deprivation paradigm (Wallace and Sakmann 2007). Second, Thompson et al. (2005) directly measured the spatial spread of sensory-evoked deoxygenation, which is a major component of the intrinsic signal, in visual thalamus, and found that the spatial decrease in oxygen signal had a half-width of 150 μm. Consistent with this tight spatial scale of signal spread, we were able to detect a relatively sharp drop off in WRA intensity at the boundary between E-row and the more medial "unresponsive zone" of S1, which does not contain neurons responsive to whisker deflection (Takashima et al. 2005). Finally, we were able to detect differences between the eccentricities of different whiskers' WRAs (e.g., E1 and C2) in control animals.

Another advantage of intrinsic imaging for measuring map plasticity derives from the finding that a large fraction of neurons in S1 of anesthetized animals exhibit very low spontaneous and whisker-evoked firing rates (Margrie et al. 2002). Because very low firing rate neurons are invisible to standard extracellular recording, map plasticity that involved silencing of previously active neurons, or activation of previously silent neurons, may be missed (Lennie 2003; Olshausen

and Field 2005; Shoham et al. 2006). In contrast, optical imaging averages activity over the entire population (Devor et al. 2003, 2005), and is therefore likely to give a more accurate global assessment of neural activity in the upper layers of cortex than could be obtained with extracellular unit recordings.

Spatial Profile of the Depression Component of Plasticity

In Hebbian synaptic plasticity, synapses strengthen between neurons with highly correlated firing, and weaken between neurons with poorly correlated firing (Hebb 1949; Stent 1973). In the dominant Hebbian (correlation-based) model for use-dependent cortical map plasticity, deprivation of a subset of inputs reduces correlated firing between deprived cortical columns and spared neighboring columns, whereas correlated firing between spared columns remains high. Thus, synaptic connections between spared and deprived columns, or between 2 deprived columns, will weaken, whereas connections between 2 spared columns will strengthen or remain strong. Consistent with this model, spared whisker representations expand preferentially into nearby spared whisker columns in adults (Diamond et al. 1993, 1994; Armstrong-James et al. 1994; Lebedev et al. 2000), and preferentially withdraw from deprived columns in young animals (Wallace and Sakmann 2007). Our data show a tendency for such withdrawal for some, but not all, spared whiskers (Figs 8*B*, 11*D*). Also consistent with this model, alteration of temporal correlations between active inputs, in the absence of deprivation, drives map plasticity that follows correlation-dependent rules and can involve reorganization of cross-columnar, horizontal projections (Löwel and Singer 1992; Wang et al. 1995; Brickley et al. 1998). However, whether these same rules are a dominant factor driving weakening of responses to deprived inputs is not known.

In D-row whisker deprivation, each deprived D-row column is directly bordered by 2 deprived D-row columns and by 2 spared C- and E-row columns. If deprivation differentially regulated firing correlations between deprived and spared columns versus between deprived and deprived columns, deprived whisker representations would be expected to withdraw anisotropically from deprived vs. spared neighbors. However, our intrinsic imaging results showed that deprived WRAs withdraw uniformly from spared vs. deprived surround columns, resulting in no change in WRA shape or alignment relative to arc or row barrel axes (Figs 5, 6). Thus, unlike expansion of spared whisker responses, contraction/weakening of deprived whisker responses occurs spatially uniformly. This suggests that differential engagement of correlation-based plasticity on cross-columnar projections is not a major contributor to weakening of deprived whisker representations. Instead, this component of plasticity may primarily reflect functional weakening or decreased density of intracolumnar synaptic connections, as has been detected in ex vivo brain slices prepared from whisker-deprived rats (Allen et al. 2003; Shepherd et al. 2003; Bender et al. 2006; Cheetham et al. 2007). Other cellular mechanisms may also be involved in induction and expression of plasticity, including changes in inhibition and intrinsic excitability (Calford 2002; Turrigiano and Nelson 2000; Foeller and Feldman 2004; Maffei et al. 2006).

Laminar Specificity of Plasticity

Deprivation reduced single-unit responses to deprived whiskers most strongly in L2/3, and more modestly in L4 (Figs 8–10). This is consistent with prior studies demonstrating that plasticity in L4 is reduced, but not completely absent, after the end of the first postnatal week (Diamond et al. 1994; Glazewski and Fox 1996; Wallace and Fox 1999; Skibinska et al. 2000; Siucinska and Kossut, 2004; Polley et al. 2004). This pattern also suggests that D-row deprivation drives plasticity at multiple synaptic loci. The modest plasticity in L4 may reflect changes at local L4 synapses or thalamocortical synapses (consistent with the observed reduction in the shortest latency spikes in L4, Suppl.Fig. 2). Deprivation at this age does not alter subcortical whisker circuits (Li et al. 1995; Glazewski et al. 1998; Wallace and Fox 1999). The more substantial plasticity in L2/3 is likely to reflect plasticity at intracortical synapses, which may include L4–L2/3 excitatory synapses, local recurrent L2/3 excitatory synapses, and/or cross-columnar synapses in L2/3, all of which are altered by deprivation of whisker rows (Finnerty et al. 1999; Allen et al. 2003; Shepherd et al. 2003; Bender et al. 2006; Cheetham et al. 2007). The known weakening of L4–L2/3 excitatory synapses and recurrent L2/3 excitatory synapses in deprived columns would provides a simple explanation for reduced transfer of whisker information from L4 to L2/3, and would predict uniform contraction of deprived whisker representations in L2/3, as observed here.

Effect of Deprivation on Spared Whisker Representations

The literature contains mixed predictions about the effect of deprivation on spared whisker representations. In older rats and mice (P28–adult), deprivation of a subset of whiskers produces strengthening and expansion of spared whisker representations (Diamond et al. 1993, 1994; Armstrong-James et al. 1992; Glazewski and Fox 1996; Wallace and Fox 1999; Polley et al. 1999; Glazewski et al. 2007). In young animals, deprivation of 3 whisker rows from P7 to 17 causes spared whisker representations to anisometrically contract away from deprived rows, rather than to expand (Wallace and Sakmann 2007). At intermediate ages, deprivation fails to drive any measurable changes in spared whisker representations (P21–31: Wallace and Sakmann 2007; P13–P30: Foeller et al. 2005). In the current study, D-row deprivation from P20 to 30 caused 1) no change in the strength of spared whisker responses in their home columns; 2) no expansion of spared whisker representations into deprived columns, and 3) mixed evidence for contraction of spared whisker representations from deprived columns—contraction was not evident from intrinsic signal imaging, but was observed for some spared whiskers in single-unit recordings in deprived columns.

Together, these findings indicate that at ~P20, deprivation weakens responses to deprived whiskers in L2/3, but that spared whisker representations show less or no plasticity, consistent with distinct molecular mechanisms for these components of plasticity (Glazewski et al. 2000; Fox 2002; Feldman and Brecht 2005).

Supplementary Material

Supplementary material can be found at: http://www.cercor.oxfordjournals.org/

Funding

National Institutes of Health (R01 NS46652); and training grant (NS07220) to P.J.D.

Notes

We thank M. Andermann, C. Moore, C. Petersen, and J. Trachtenberg for advice on intrinsic imaging and K. Bender for helpful discussions.

Conflict of Interest: None declared.

Address correspondence to Dan Feldman, PhD, Department of Molecular and Cell Biology, 142 LSA #3200, UC Berkeley, Berkeley, CA 94720-3200, USA. Email: dfeldman@berkeley.edu.

References

Allen CB, Celikel T, Feldman DE. 2003. Long-term depression induced by sensory deprivation during cortical map plasticity in vivo. Nat Neurosci. 6(3):291–299.

Armstrong-James M, Diamond ME, Ebner FF. 1994. An innocuous bias in whisker use in adult rats modifies receptive fields of barrel cortex neurons. J Neurosci. 14(11 Pt 2):6978–6991.

Armstrong-James M, Fox K. 1987. Spatiotemporal convergence and divergence in the rat S1 "barrel" cortex. J Comp Neurol. 263(2): 265–281.

Armstrong-James M, Fox K, Das-Gupta A. 1992. Flow of excitation within rat barrel cortex on striking a single vibrissa. J Neurophysiol. 68(4):1345–1358.

Bender KJ, Allen CB, Bender VA, Feldman DE. 2006. Synaptic basis for whisker deprivation-induced synaptic depression in rat somatosensory cortex. J Neurosci. 26(16):4155–4165.

Bender KJ, Rangel J, Feldman DE. 2003. Development of columnar topography in the excitatory layer 4 to layer 2/3 projection in rat barrel cortex. J Neurosci. 23(25):8759–8770.

Bernardo KL, McCasland JS, Woolsey TA, Strominger RN. 1990. Local intra- and interlaminar connections in mouse barrel cortex. J Comp Neurol. 291:231–255.

Brecht M, Roth A, Sakmann B. 2003. Dynamic receptive fields of reconstructed pyramidal cells in layers 3 and 2 of rat somatosensory barrel cortex. J Physiol. 553:243–265.

Brickley SG, Dawes EA, Keating MJ, Grant S. 1998. Synchronizing retinal activity in both eyes disrupts binocular map development in the optic tectum. J Neurosci. 18(4):1491–1504.

Buonomano DV, Merzenich MM. 1998. Cortical plasticity: from synapses to maps. Annu Rev Neurosci. 21:149–186.

Calford MB. 2002. Dynamic representational plasticity in sensory cortex. Neuroscience. 111(4):709–738.

Cang J, Kalatsky VA, Löwel S, Stryker MP. 2005. Optical imaging of the intrinsic signal as a measure of cortical plasticity in the mouse. Vis Neurosci. 22(5):685–691.

Celikel T, Szostak VA, Feldman DE. 2004. Modulation of spike timing by sensory deprivation during induction of cortical map plasticity. Nat Neurosci. 7(5):534–541.

Cheetham CE, Hammond MS, Edwards CE, Finnerty GT. 2007. Sensory experience alters cortical connectivity and synaptic function site specifically. J Neurosci. 27(13):3456–3465.

Chen-Bee CH, Polley DB, Brett-Green B, Prakash N, Kwon MC, Frostig RD. 2000. Visualizing and quantifying evoked cortical activity assessed with intrinsic signal imaging. J Neurosci Methods. 97(2):157–173.

Crair MC, Ruthazer ES, Gillespie DC, Stryker MP. 1997a. Relationship between the ocular dominance and orientation maps in visual cortex of monocularly deprived cats. Neuron. 19(2):307–318.

Crair MC, Ruthazer ES, Gillespie DC, Stryker MP. 1997b. Ocular dominance peaks at pinwheel center singularities of the orientation map in cat visual cortex. J Neurophysiol. 77(6):3381–3385.

Devor A, Dunn AK, Andermann ML, Ulbert I, Boas DA, Dale AM. 2003. Coupling of total hemoglobin concentration, oxygenation, and neural activity in rat somatosensory cortex. Neuron. 39(2): 353–359.

Devor A, Ulbert I, Dunn AK, Narayanan SN, Jones SR, Andermann ML, Boas DA, Dale AM. 2005. Coupling of the cortical hemodynamic response to cortical and thalamic neuronal activity. Proc Natl Acad Sci USA. 8102(10):3822–3827.

Diamond ME, Armstrong-James M, Ebner FF. 1993. Experience-dependent plasticity in adult rat barrel cortex. Proc Natl Acad Sci USA. 90(5):2082–2086.

Diamond ME, Huang W, Ebner FF. 1994. Laminar comparison of somatosensory cortical plasticity. Science. 265(5180):1885–1888.

Drew PJ, Feldman DE. 2007. Representation of moving wavefronts of whisker deflection in rat somatosensory cortex. J Neurophysiol. 98(3):1566–1580.

Dubroff JG, Stevens RT, Hitt J, Maier DL, McCasland JS, Hodge CJ. 2005. Use-dependent plasticity in barrel cortex: intrinsic signal imaging reveals functional expansion of spared whisker representation into adjacent deprived columns. Somatosens Mot Res. 22(1–2):25–35.

Erchova IA, Lebedev MA, Diamond ME. 2002. Somatosensory cortical neuronal population activity across states of anaesthesia. Eur J Neurosci. 15:744–752.

Fee MS, Mitra PP, Kleinfeld D. 1996. Automatic sorting of multiple unit neuronal signals in the presence of anisotropic and non-Gaussian variability. J Neurosci Methods. 69(2):175–188.

Feldman DE, Brecht M. 2005. Map plasticity in somatosensory cortex. Science. 310(5749):810–815.

Finnerty GT, Roberts LS, Connors BW. 1999. Sensory experience modifies the short-term dynamics of neocortical synapses. Nature. 400:367–371.

Foeller E, Celikel T, Feldman DE. 2005. Inhibitory sharpening of receptive fields contributes to whisker map plasticity in rat somatosensory cortex. J Neurophysiol. 94(6):4387–4400.

Foeller E, Feldman DE. 2004. Synaptic basis for developmental plasticity in somatosensory cortex. Curr Opin Neurobiol. 14(1):89–95.

Fox K. 1992. A critical period for experience-dependent synaptic plasticity in rat barrel cortex. J Neurosci. 12(5):1826–1838.

Fox K. 2002. Anatomical pathways and molecular mechanisms for plasticity in the barrel cortex. Neuroscience. 111(4):799–814.

Fox K, Glazewski S, Chen CM, Silva A, Li X. 1996. Mechanisms underlying experience-dependent potentiation and depression of vibrissae responses in barrel cortex. J Physiol Paris. 90:263–269.

Gabernet L, Jadhav SP, Feldman DE, Carandini M, Scanziani M. 2005. Somatosensory integration controlled by dynamic thalamocortical feed-forward inhibition. Neuron. 48(2):315–327.

Gilbert CD. 1998. Adult cortical dynamics. Physiol Rev. 78(2): 467–485.

Glazewski S, Benedetti BL, Barth AL. 2007. Ipsilateral whiskers suppress experience-dependent plasticity in the barrel cortex. J Neurosci. 27(14):3910–3920.

Glazewski S, Chen CM, Silva A, Fox K. 1996. Requirement for alpha-CaMKII in experience-dependent plasticity of the barrel cortex. Science. 272:421–423.

Glazewski S, Fox K. 1996. Time course of experience-dependent synaptic potentiation and depression in barrel cortex of adolescent rats. J Neurophysiol. 75(4):1714–1729.

Glazewski S, Giese KP, Silva A, Fox K. 2000. The role of alpha-CaMKII autophosphorylation in neocortical experience-dependent plasticity. Nat Neurosci. 3(9):911–918.

Grinvald A, Lieke E, Frostig RD, Gilbert CD, Wiesel TN. 1986. Functional architecture of cortex revealed by optical imaging of intrinsic signals. Nature. 324(6095):361–364.

Glazewski S, McKenna M, Jacquin M, Fox K. 1998. Experience-dependent depression of vibrissae responses in adolescent rat barrel cortex. Eur J Neurosci. 10(6):2107–2116.

Gurden H, Uchida N, Mainen ZF. 2006. Sensory-evoked intrinsic optical signals in the olfactory bulb are coupled to glutamate release and uptake. Neuron. 52(2):335–345.

Jacob V, Brasier DJ, Erchova I, Feldman D, Shulz DE. 2007. Spike timing-dependent synaptic depression in the in vivo barrel cortex of the rat. J Neurosci. 27(6):1271–1284.

Kim U, Ebner FF. 1999. Barrels and septa: separate circuits in rat barrel field cortex. J Comp Neurol. 408(4):489–505.

Kossut M. 1989. Experience-dependent changes in function and anatomy of adult barrel cortex. Exp Brain Res. 123(1–2):110–116.

Lebedev MA, Mirabella G, Erchova I, Diamond ME. 2000. Experience-dependent plasticity of rat barrel cortex: redistribution of activity across barrel-columns. Cereb Cortex. 10(1):23–31.

Lennie P. 2003. The cost of cortical computation. Curr Biol. 13(6): 493–497.

Li X, Glazewski S, Lin X, Elde R, Fox K. 1995. Effect of vibrissae deprivation on follicle innervation, neuropeptide synthesis in the trigeminal ganglion, and S1 barrel cortex plasticity. J Comp Neurol. 357(3):465–481.
Löwel S, Singer W. 1992. Selection of intrinsic horizontal connections in the visual cortex by correlated neuronal activity. Science. 255(5041):209–212.
Maffei A, Nataraj K, Nelson SB, Turrigiano GG. 2006. Potentiation of cortical inhibition by visual deprivation. Nature. 443(7107):81–84.
Margrie TW, Brecht M, Sakmann B. 2002. In vivo, low-resistance, whole-cell recordings from neurons in the anaesthetized and awake mammalian brain. Pflugers Arch. 444(4):491–498.
Masino SA. 2003. Quantitative comparison between functional imaging and single-unit spiking in rat somatosensory cortex. J Neurophysiol. 89(3):1702–1712.
Masino SA, Kwon MC, Dory Y, Frostig RD. 1993. Characterization of functional organization within rat barrel cortex using intrinsic signal optical imaging through a thinned skull. Proc Natl Acad Sci USA. 90(21):9998–10002.
Mayhew JE, Askew S, Zheng Y, Porrill J, Westby GW, Redgrave P, Rector DM, Harper RM. 1996. Cerebral vasomotion: a 0.1-Hz oscillation in reflected light imaging of neural activity. Neuroimage. 4(3 Pt 1):183–193.
Nemoto M, Sheth S, Guiou M, Pouratian N, Chen JW, Toga AW. 2004. Functional signal- and paradigm-dependent linear relationships between synaptic activity and hemodynamic responses in rat somatosensory cortex. J Neurosci. 24(15):3850–3861.
Olshausen BA, Field DJ. 2005. How close are we to understanding v1? Neural Comput. 17(8):1665–1699.
Peterson BE, Goldreich D, Merzenich MM. 1998. Optical imaging and electrophysiology of rat barrel cortex. I. Responses to small single-vibrissa deflections. Cereb Cortex. 8:173–183.
Petersen CC. 2003. The barrel cortex—integrating molecular, cellular and systems physiology. Pflugers Arch. 447(2):126–134.
Petersen CC, Grinvald A, Sakmann B. 2003. Spatiotemporal dynamics of sensory responses in layer 2/3 of rat barrel cortex measured in vivo by voltage-sensitive dye imaging combined with whole-cell voltage recordings and neuron reconstructions. J Neurosci. 23(4):1298–1309.
Polley DB, Chen-Bee CH, Frostig RD. 1999. Two directions of plasticity in the sensory-deprived adult cortex. Neuron. 24(3):623–637.
Polley DB, Kvasnak E, Frostig RD. 2004. Naturalistic experience transforms sensory maps in the adult cortex of caged animals. Nature. 429(6987):67–71.
Ratzlaff EH, Grinvald A. 1991. A tandem-lens epifluorescence macroscope: hundred-fold brightness advantage for wide-field imaging. J Neurosci Methods. 36(2-3):127–137.
Sengpiel F, Baddeley RJ, Freeman TC, Harrad R, Blakemore C. 1998. Different mechanisms underlie three inhibitory phenomena in cat area 17. Vision Res. 38(14):2067–2080.
Shepherd GM, Pologruto TA, Svoboda K. 2003. Circuit analysis of experience-dependent plasticity in the developing rat barrel cortex. Neuron. 38(2):277–289.
Sheth BR, Moore CI, Sur M. 1998. Temporal modulation of spatial borders in rat barrel cortex. J Neurophysiol. 79(1):464–470.
Shoham S, O'Connor DH, Segev R. 2006. How silent is the brain: is there a "dark matter" problem in neuroscience? J Comp Physiol A Neuroethol Sens Neural Behav Physiol. 192(8):777–784.
Simons DJ. 1978. Response properties of vibrissa units in rat SI somatosensory neocortex. J Neurophysiol. 41(3):798–820.
Simons DJ, Land PW. 1987. Early experience of tactile stimulation influences organization of somatic sensory cortex. Nature. 326(6114):694–697.
Siucinska E, Kossut M. 2004. Experience-dependent changes in cortical whisker representation in the adult mouse: a 2-deoxyglucose study. Neuroscience. 127(4):961–971.
Skibinska A, Glazewski S, Fox K, Kossut M. 2000. Age-dependent response of the mouse barrel cortex to sensory deprivation: a 2-deoxyglucose study. Exp Brain Res. 132(1):134–138.
Smith SL, Trachtenberg JT. 2007. Experience-dependent binocular competition in the visual cortex begins at eye opening. Nat Neurosci. 10(3):370–375.
Song S, Abbott LF. 2001. Cortical development and remapping through spike timing-dependent plasticity. Neuron. 32(2):339–350.
Swadlow HA. 1989. Efferent neurons and suspected interneurons in S-1 vibrissa cortex of the awake rabbit: receptive fields and axonal properties. J Neurophysiol. 62(1):288–308.
Stent GS. 1973. A physiological mechanism for Hebb's postulate of learning. Proc Natl Acad Sci USA. 70(4):997–1001.
Takashima I, Kajiwara R, Iijima T. 2005. Voltage-sensitive dye imaging of intervibrissal fur-evoked activity in the rat somatosensory cortex. Neurosci Lett. 381(3):258–263.
Thompson JK, Peterson MR, Freeman RD. 2005. Separate spatial scales determine neural activity-dependent changes in tissue oxygen within central visual pathways. J Neurosci. 25(39):9046–9058.
Ts'o DY, Frostig RD, Lieke EE, Grinvald A. 1990. Functional organization of the primate visual cortex revealed by high-resolution optical imaging of intrinsic signals. Science. 249:417–420.
Turrigiano GG, Nelson SB. 2000. Hebb and homeostasis in neuronal plasticity. Curr Opin Neurobiol. 10(3):358–364.
Wallace DJ, Sakmann B. 2007. Plasticity of representational maps in somatosensory cortex observed by in vivo voltage-sensitive dye imaging. Cereb Cortex. 10.1093.
Wallace H, Fox K. 1999. The effect of vibrissa deprivation pattern on the form of plasticity induced in rat barrel cortex. Somatosens Mot Res. 16(2):122–138.
Wallace H, Glazewski S, Liming K, Fox K. 2001. The role of cortical activity in experience-dependent potentiation and depression of sensory responses in rat barrel cortex. J Neurosci. 21(11): 3881–3894.
Wang X, Merzenich MM, Sameshima K, Jenkins WM. 1995. Remodelling of hand representation in adult cortex determined by timing of tactile stimulation. Nature. 378(6552):71–75.
Welker W. 1964. Analysis of sniffing of the albino rat. Behavior. 22: 223–244.